Title
Somatodendritic Expression of JAM2 Inhibits Oligodendrocyte Myelination

Author
Redmond, Stephanie Anne

Publication Date
2016

Peer reviewed|Thesis/dissertation

Somatodendritic Expression of JAM2 Inhibits Oligodendrocyte Myelination

by

Stephanie Anne Redmond

DISSERTATION

Submitted in partial satisfaction of the requirements for the degree of

DOCTOR OF PHILOSOPHY

in

Neuroscience

in the

GRADUATE DIVISION

[redacted]

Dedication

For my family, without whose continued and unending support this project and my degree never would have been possible.

And for Jonah Chan, who thankfully never really believed I was just a physicist.

Acknowledgements

I would like to thank the members of the Chan Lab and the Neuroscience Graduate Program for their personal and scientific support during my time at UCSF. I would also like to thank my thesis committee for their time and feedback over the years that was critical for this project to come to fruition: Drs. Sam Pleasure (chair), Yuh-Nung Jan, David Rowitch, Anna Molofsky and Daniela Kaufer.

Chapter One

The text of this thesis chapter is a reprint of the material as it appears in *Remodeling Myelination: Implications for Mechanisms of Neural Plasticity* (Chang et al., 2016). Author contributions: K.-J.C., S.A.R. and J.R.C. wrote the paper.

This review was supported by the NMSS Research Grants (RG4541A3 and RG5203A4), NIH/NINDS (R01NS062796), and the Rachleff Endowment to JRC. SAR is supported by NIH/NINDS NRSA (F31NS081905). The EM picture in Fig. 1-1 is by courtesy of Dr. Keiichiro Susuki at Wright State University with the technical assistance by Debra Townley and support from the Integrated Microscopy Core at Baylor College of Medicine with funding from the NIH (HD007495, DK56338, and CA125123), the Dan L. Duncan Cancer Center, and the John S. Dunn Gulf Coast Consortium for Chemical Genomics. We thank Pei-Jung Lee for her insight, creativity and efforts in making all the illustrations. We also thank Dr. Ari J. Green and the members of the Chan laboratory for critical reading of the manuscript and insightful comments. We respectfully apologize to colleagues whose relevant work was not discussed due to space limitations.

Chapter Two

The text of this thesis chapter is a reprint of the material as it appears in *Somatodendritic Expression of JAM2 Inhibits Oligodendrocyte Myelination* (Redmond et al., 2016). Author

Contributions: S.A.R., F.M., Y.E.-E., L.A.O., D.L., Y.-A.A.S., J.N.K. and J.R.C. performed experiments. Y.E.-E., M.A.L., E.P. and J.R.C. provided reagents. S.A.R., F.M., Y.E.-E., L.A.O., Y.-A.A.S., J.N.K., D.A.L., E.P. and J.R.C. provided intellectual contributions. S.A.R., D.L. and J.R.C. analyzed the data. S.A.R. and J.R.C. wrote the paper.

We thank Dr. W.B. Stallcup and Dr. L.F. Reichardt for antibodies, M.L. Wong for ultrathin sectioning of electron microscopy samples, J. Wong for semi-thin sectioning and toluidine blue staining (Gladstone Institutes Electron Microscopy Core, San Francisco, CA). We also thank Dr. K.-J. Chang for technical assistance, Dr. S.Y.C. Chong for efforts on development of SCN culture conditions, members of the Chan Laboratory for critical reading of the manuscript, and the UCSF Clinical and Translational Science Institute, for biostatistics consultation (NIH UL1 TR000004). This work was supported by NMSS Research Grants (RG4541A3 and RG5203A4), NIH/NINDS (R01NS062796, R01NS097428) and the Rachleff Family Professorship to J.R.C.; NIH/NINDS (R01NS50220), and the Dr. Miriam and Sheldon G. Adelson Medical Research Foundation, the Incumbent of the Hanna Hertz Professorial Chair for Multiple Sclerosis and Neuroscience to E.P.; NSERC PGS D to L.A.O.; and NIH/NINDS Ruth L. Kirschstein NRSA (F31NS081905) to S.A.R.

Chapter Three

The text of this thesis chapter is a reprint of the material as it appears in *Revitalizing Remyelination—the Answer Is Circulating* (Redmond and Chan, 2012). Author contributions: S.A.R. and J.R.C. wrote the paper.

We thank members of the Chan Laboratory and O. Ahmed for critical reading of the manuscript. Figure artwork credit: Y. Hammond, Science.

Table of Contents

List of Figures

Abstract

The advent of myelin was instrumental in advancing the nervous system during vertebrate evolution. With more rapid and efficient communication between neurons, faster and more complex computation could be performed in a given time and space. Our knowledge of how myelin-forming oligodendrocytes select and wrap axons has been limited by insufficient spatial and temporal resolution. By virtue of recent technological advances, significant progress has clarified longstanding controversies in the field. Here, we review insights into myelination, from target selection to axon wrapping and membrane compaction, and discuss how understanding these processes has unexpectedly opened new avenues of insight into myelination-centered mechanisms of neural plasticity.

Myelination occurs selectively around neuronal axons to increase the efficiency and velocity of action potentials. While oligodendrocytes are capable of myelinating permissive structures in the absence of molecular cues, structurally permissive neuronal somata and dendrites remain unmyelinated. Utilizing a purified spinal cord neuron-oligodendrocyte myelinating coculture system, we demonstrate that disruption of dynamic neuron-oligodendrocyte signaling by chemical crosslinking results in aberrant myelination of the somatodendritic compartment of neurons. We hypothesize that an inhibitory somatodendritic cue is necessary to prevent non-axonal myelination. Using next-generation sequencing and candidate profiling, we identify neuronal Junction Adhesion Molecule 2 (JAM2) as an inhibitory myelin-guidance molecule. Taken together, our results demonstrate that the somatodendritic compartment directly inhibits myelination, and suggest a model in which broadly indiscriminate myelination is tailored by inhibitory signaling to meet local myelination requirements.

Efficient myelin repair after demyelinating injury is thought to prevent loss of neural function and prevent neurodegeneration. Within the central nervous system, the capacity for myelin repair theoretically exists. Oligodendrocyte precursor cells (OPCs) are capable of differentiating into myelinating oligodendrocytes throughout life. However, many demyelinated lesions fail to remyelinate, despite the presence of OPCs and even differentiated oligodendrocytes within demyelinated areas. It has been recently shown that more efficient myelin debris removal promotes remyelination. Myelin guidance molecules at work during development to ensure correct myelination patterns, like inhibitory JAM2, may play significant roles in preventing efficient myelin repair in disease. Identifying more myelin guidance molecules may represent a novel avenue to develop new remyelination therapies.

Chapter One: Remodeling Myelination: Implications for Mechanisms of Neural Plasticity

Abstract

One of the most significant paradigm shifts in membrane remodeling is the emerging view that membrane transformation is not exclusively controlled by cytoskeletal rearrangement, but also by biophysical constraints, adhesive forces, membrane curvature and compaction. One of the most exquisite examples of membrane remodeling is myelination. The advent of myelin was instrumental in advancing the nervous system during vertebrate evolution. With more rapid and efficient communication between neurons, faster and more complex computation could be performed in a given time and space. Our knowledge of how myelin-forming oligodendrocytes select and wrap axons has been limited by insufficient spatial and temporal resolution. By virtue of recent technological advances, significant progress has clarified longstanding controversies in the field. Here, we review insights into myelination, from target selection to axon wrapping and membrane compaction, and discuss how understanding these processes has unexpectedly opened new avenues of insight into myelination-centered mechanisms of neural plasticity.

Introduction

As the nervous system grew more computationally powerful and increasingly complex, the evolution of glial myelination allowed jawed vertebrates to overcome the pressure of increasing nervous system size for faster conduction speed and dramatically advanced the functional efficiency and complexity of the nervous system (Hartline and Colman, 2007; Zalc et al., 2008). Myelin sheaths are made of glial plasma membranes that wrap around axons in a multi-lamellar compact spiral (Fig. 1a,b) (Bunge et al., 1962; Geren, 1954). These compact membrane layers serve as an insulator by increasing the resistance and decreasing the capacitance across the axonal membrane. Myelinating glia further potentiate rapid saltatory conduction by actively clustering voltage-gated sodium channels at the gaps between myelin sheaths (Eshed-Eisenbach and Peles, 2013; Hartline and Colman, 2007; Normand and Rasband, 2015), called nodes of Ranvier (Fig. 1a,c). Myelin sheath thickness, length and axonal coverage patterns can affect the conduction velocity of action potentials (Babbs and Shi, 2013; Waxman, 1980, 1997). Additionally, nodal length and channel density at the node may also influence the efficiency and velocity of the action potential. Perhaps unsurprisingly then, much attention has been devoted to exploring the possibility that neuronal activity may influence myelination by oligodendroglia and regulate these parameters to modulate the conduction velocity in each underlying axon. It is an appealing concept that such dynamic myelination throughout the CNS might provide an additional mechanism for neural circuit plasticity by modulating timing and coordinating network synchrony and oscillations (Fields, 2008; Pajevic et al., 2014). Without understanding myelination, we cannot fully appreciate how the nervous system develops and functions.

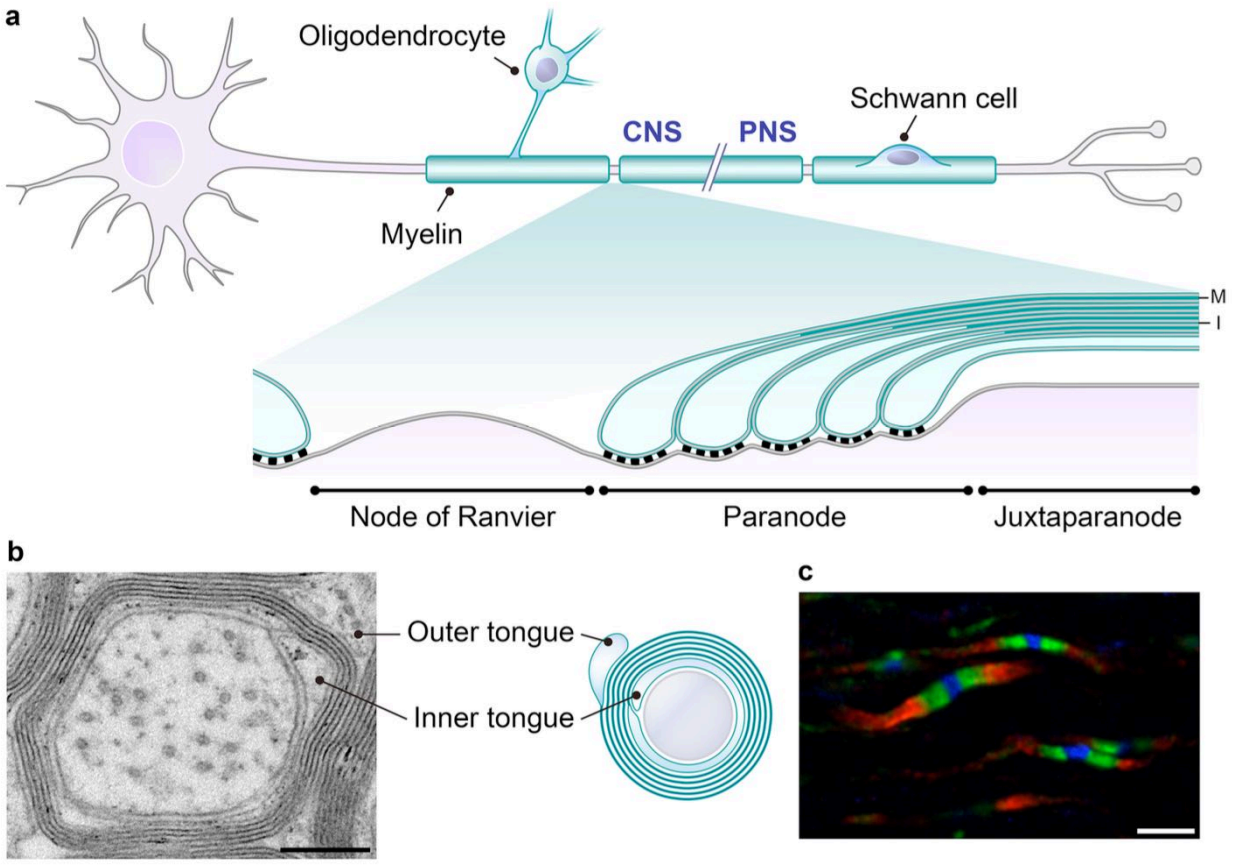

Figure 1-1 | Structure of myelin and molecular domains along myelinated axons.

Schema of a neuron and the myelin sheaths along its axon. Myelin sheaths are made by oligodendrocytes in the CNS and by Schwann cells in the PNS. A single oligodendrocyte can generate multiple myelin sheaths, whereas an individual Schwann cell only makes one. The close-up view shows the ultrastructure around the node of Ranvier. Glial membranes at the ends of the sheaths are attached to the axonal membrane flanking the node, forming paranodes. Paranodal loops contain cytoplasm and are not compacted. Neuron-glia interactions at paranodes form paranodal axoglial junctions with the characteristic electron-dense transverse bands under EM. (b) An EM image from the cross section of an adult mouse optic nerve and its illustration. The major dense lines ("M" in a) are clearly visualized, but the intraperiod lines ("I" in a) are not obvious under this magnification. The ends of the myelin spiral are the outer and inner tongues, which contain cytoplasm and are not compacted. (c) Immunostaining of a postnatal day 22 mouse optic nerve shows three molecular domains around nodes of Ranvier. Blue: nodes by βIV spectrin; green: paranodal junctions by Caspr; red: juxtaparanodes by potassium channel Kv1.2. The majority of the myelinated region is between two juxtaparanodes and not visualized here. Scale bars: 200 nm (b); 3 μm (c). The illustration (a) was adapted from (Chang and Rasband, 2013) with permission from Elsevier. For simplicity, the illustration (b) does not follow a regular g-ratio.

Through recent advancement in technologies, our understanding of how myelin is formed and regulated has been drastically enhanced. In this review, we focus on the most recent findings that together draw a current mechanistic sketch of how oligodendrocytes select their targets, elaborate spiral layers of myelin membranes and how these membrane layers compact to form mature sheaths. Finally, we take these mechanistic insights and consider how the formation and even remodeling of myelin may be harnessed as a new tool contributing to neural plasticity in the CNS.

Where to wrap? – The biophysical and molecular settings

There is a close correlation between the myelination status of a CNS axon and whether or not it is above a threshold diameter (≥ 0.2-0.4 μm) (Hildebrand et al., 1993; Wang et al., 2008). What is the instructive signal that dictates this diameter requirement? Is it simply a matter of permissive geometry or is it transduced by dynamic molecular signaling? These questions have been addressed in the PNS, where Schwann cell ErbB2/ErbB3 receptors sense axonal levels of neuregulin 1 type III (Nrg1-III). Although it remains unclear how the level of Nrg1-III is normally regulated to precisely reflect an axon's diameter, suprathreshold Nrg1/ErbB signaling is the well-accepted determinant essential for myelination in the PNS, which can even override the biophysical parameter of axon diameter (Mei and Nave, 2014; Salzer, 2015). Surprisingly, Nrg1/ErbB signaling is largely dispensable for CNS myelination (Brinkmann et al., 2008), and several observations now collectively indicate that oligodendrocytes may not need an instructive signal to initiate myelination. Unlike Schwann cells, oligodendrocytes can differentiate and spread membrane sheets containing myelin proteins and lipids in the absence of neurons in vitro (Aggarwal et al., 2011; Mirsky et al., 1980). Oligodendrocytes myelinate paraformaldehyde-fixed axons, suggesting dynamic neuron-glial interactions are not required for CNS myelination (Rosenberg et al., 2008). More recently, it was demonstrated that oligodendrocytes can even

myelinate electrospun nanofibers above a threshold diameter between 0.3 and 0.4 μm (Lee et al., 2012), comparable to observed myelinated axon calibers in vivo, where the frequency of myelinated axons below 0.3 μm in diameter is extremely low (Hildebrand et al., 1993; Wang et al., 2008). These findings indicate that a sufficiently small target diameter may represent a biophysical barrier to myelination of small-diameter axons.

Taken together, oligodendrocytes appear to exhibit intrinsically broad target selection and wrapping activities, defined at least in part by unknown molecular sensors of fiber curvature. However, highly stereotyped spatiotemporal myelination patterns observed in the developing CNS (Brody et al., 1987; Foran and Peterson, 1992; Kinney et al., 1988) leave plenty of room for molecular regulation and fine-tuning of these 'default' settings to better suit local needs in the oligodendrocyte microenvironment. Take, for instance, non-axonal structures such as neuronal dendrites and somata, or existing myelinated axons that meet threshold diameter requirements, yet are overwhelmingly avoided by differentiating oligodendrocytes. Inhibitory signaling to oligodendrocytes could curb myelination of these structures. While not absolutely required for selection and wrapping, the observation that oligodendrocytes prefer axons to nanofibers (unpublished observations by SAR and JRC) suggests the existence of attractive cues on axons. For instance, a cell adhesion molecule could be considered attractive if it preferentially stabilizes the initial contact between the oligodendrocyte and axon, resulting in an increased likelihood for subsequent myelination. Interestingly, both myelinated and unmyelinated axons of near-threshold diameters (0.2-0.8 μm) are observed in the CNS (Hildebrand et al., 1993; Wang et al., 2008). This suggests that the intrinsic property of oligodendrocytes can be adjusted by other undefined fine-tuning cues and mechanisms that induce oligodendrocytes to myelinate sub-threshold axons and prevent wrapping of otherwise biophysically permissive ones. Such cues include attractive and repulsive molecules, which could potentially be regulated in a neuronal activity-dependent manner. Identification of these molecules and how they function has been of

substantial interest in the myelin field (Piaton et al., 2010; Taveggia et al., 2010). Recently, reconstruction of large EM data sets revealed scattered examples of long unmyelinated stretches of otherwise myelinated axons in the cortex (Tomassy et al., 2014). This suggests that even along the very same axon, differential regulation of myelination might exist. It is tempting to speculate that graded expression and localization of repulsive and attractive cues along an axon could pattern myelin sheath length and spacing, which in turn can affect action potential conduction velocity and the timing of neurotransmitter release to postsynaptic targets. These parameters could vary within a given neural circuit to establish functionally desirable synchrony and oscillation patterns, and could be remodeled in the adult as an additional mechanism contributing to neural plasticity.

Transforming a cellular process into a spiraled sheet

Formation of myelin by wrapping glial plasma membranes around axons is one of the most remarkable biological events in membrane remodeling. To generate a 100 µm-long myelin sheath of ten spiral wraps around a one micron-diameter axon, myelinating glia need to generate over 6,400 μm^2 of membrane! However, the delicate and elaborate nature of compact myelin and technical difficulties in resolving it to the nanometer level dramatically hinders our detailed understanding of the wrapping process. Even Ramón y Cajal misinterpreted myelin as an axonal adjunct “entirely foreign to Schwann cells” in the PNS (Ramón y Cajal, 1928).

Our understanding of the active wrapping process during myelination initiated with studies on Schwann cells (Geren, 1954; Robertson, 1955). Continuous observation of the myelination process in culture by light microscopy and subsequent electron microscopy (EM) analysis excluded a cell body-driven wrapping mechanism (Bunge et al., 1989). These observations resulted in the ‘carpet crawler’ model of myelination where wrapping occurs by the inward ‘crawling’ of the inner tongue around the axonal circumference, leaving a trail of the spirally

extending myelin membrane sheet behind. This classic model would predict that the front of the inner tongue advances as a straight line along the axon during wrapping, resulting in a homogeneous number of wraps along the length of the forming sheath. Although the carpet crawler model may be still extrapolated to CNS myelination, it has turned out to be inconsistent with some early EM observations. For example, the number of wraps along the length was found to be greater in the middle and fewer toward the ends of a forming sheath (Fraher, 1973, 1978; Webster, 1971). This suggests the front of the inner tongue advances as a convex curve (Fig. 2), instead of a straight line. It also suggests that the radial growth (increase in wraps) and longitudinal growth (membrane sheet widening) take place simultaneously. To fill the gap between the carpet crawler model and observations like variable wrap number, more recent work utilizing cell culture systems, fluorescent proteins, as well as light and electron microscopy led to the 'ofiomosaic' (Ioannidou et al., 2012) and 'liquid croissant' (Sobottka et al., 2011) models. Both models propose very different pictures of early wrapping events, and a fundamental difference among all three models lies in the way the membrane extends: from the innermost layer (carpet crawler), from the outermost layer (liquid croissant), or through lateral expansion of a glial process spiraling along an axon (ofiomosaic). Efforts to reconcile the different models and resolve the manner in which the membrane remodels during wrapping were hindered by limitations in spatial resolution of light microscopy, cell culture conditions, selective membrane labeling and EM artifacts produced throughout sample processing.

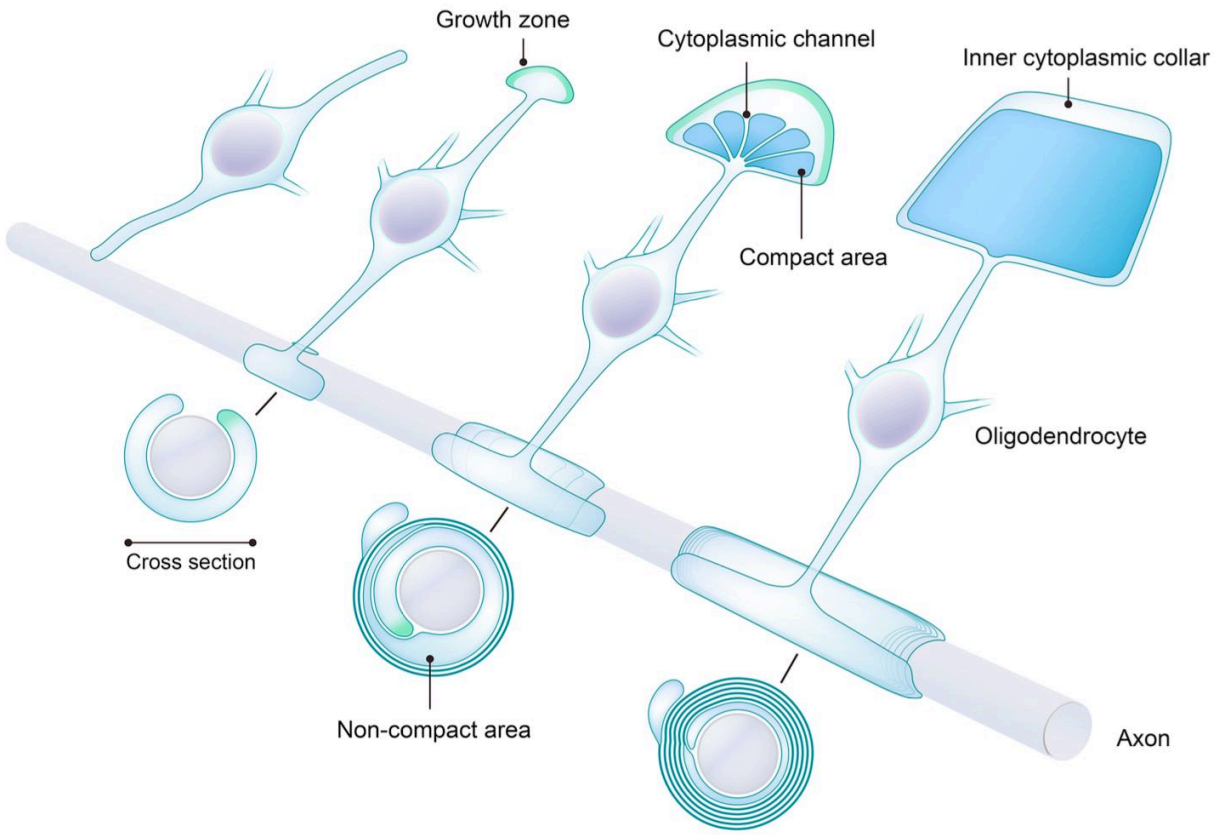

Figure 1-2 | The current model of myelination in the CNS.

From left-to-right: A newly-differentiated oligodendrocyte extends a process to an unmyelinated axon. After contacting the axon, it starts wrapping by spreading its membrane. The growth zone for active membrane incorporation is shown in green. The myelin membrane grows both radially (more wraps) and longitudinally (longer sheath). When there are about three layers of myelin membrane, the intracellular compaction initiates from the outermost layer toward the inner layers, preserving uncompacted cytoplasmic channels for material transport between the oligodendrocyte process and the growth zone. If a mature myelin sheath were unrolled from the axon, it would consist of a trapezoid of compacted membrane lined with a continuous cytoplasmic collar. When coiled around the axon, the lateral cytoplasmic collars form loops located at the paranodes (see also Fig. 1-1a). The corresponding cross sections are displayed below the axon. An illustration of a virtually unrolled myelin sheet at each stage is shown at the top process of the oligodendrocyte. Myelin retraction may occur during the active myelination process (represented by one missing process in the right-most oligodendrocyte). The illustration was adapted from (Snaidero et al., 2014) with permission of Elsevier.

Recent breakthrough studies have taken definitive and narrow approaches to closely describe both early myelination events and the elaboration of the growing myelin sheath. The advent of high-pressure freezing with subsequent freeze substitution preserves native tissue architecture, eliminating many of the EM artifacts associated with fixation and processing (Möbius et al., 2010). When combined with focused ion beam milling-coupled scanning EM for serial block-face imaging, the methods provide high-resolution three-dimensional images of nanoscale structures (Peddie and Collinson, 2014). The additional use of high-resolution in vivo imaging of transgenic zebrafish larvae combined to generate the most current and complete model of the myelination process to date (Fig. 2) (Czopka et al., 2013; Snaidero et al., 2014). Exploratory oligodendrocyte processes were found to transform into short but elongating myelin sheaths (Czopka et al., 2013). The number of wraps is greatest at the site where the oligodendrocyte process is connected to the growing myelin sheath and gradually decreases toward the ends (Snaidero et al., 2014), consistent with the early EM findings (Fraher, 1973, 1978; Webster, 1971). The longitudinal length of the membrane lamellae is shortest for the innermost layer and gradually longer toward the outermost one; the inner layers are covered completely by the respective outer ones. Thus, the inner tongue winds the axon spirally during active wrapping and may account for the helical coil patterns observed by light microscopy underlying the ofiomosaic and liquid croissant models. In addition, each layer has cytoplasm-containing edges, which are part of the continuous cytoplasmic collar of the membrane sheet and are always attached to the axon. As development progresses, these lateral cytoplasmic loops move toward the edges of the myelin sheath while each layer is extending longitudinally, and finally meet and align as paranodal loops (Figs. 1a and 2).

Where and how new myelin membranes are incorporated into the growing myelin sheath had not been experimentally demonstrated previously. Localization of newly synthesized vesicular

stomatitis virus glycoprotein G (VSV-G) was used as a readout of new membrane deposition in infected oligodendroglia. As it turned out, new VSV-G accumulated at the inner tongue, reinforcing the idea that the inner tongue is the primary growth zone in growing myelin sheaths (Snaidero et al., 2014). Interestingly, flanked by already compacted areas, transient cytoplasmic channels containing vesicular structures were preserved in CNS myelin with the high-pressure freezing EM techniques (Snaidero et al., 2014). These findings suggest that to fuel membrane growth, the cytoplasmic channels serve as the throughways embedded in compact areas to deliver new membranes in vesicles to the inner tongue (Fig. 2). It is noteworthy that these channels gradually close as compaction spreads during development, but can be re-formed in existing myelin sheaths that are stimulated to add more myelin wraps (Snaidero et al., 2014). Then, what is the driving force that powers membrane growth in between the axon and the previous myelin layers? Intriguingly, two recent studies revealed that actin cytoskeleton dynamics is utilized by oligodendrocytes to push the inner tongues forward (Nawaz et al., 2015; Zuchero et al., 2015). Actin filaments were found to be present in the growing myelin sheaths but depolymerized in the mature compact myelin (Nawaz et al., 2015; Snaidero et al., 2014; Zuchero et al., 2015). Studies using cultured oligodendrocytes showed that actin filament depolymerization releases the membrane surface tension and promotes membrane spreading (Nawaz et al., 2015; Zuchero et al., 2015). Pharmacological treatment inducing actin depolymerization facilitated myelin wrapping in the mouse spinal cords (Zuchero et al., 2015). Furthermore, the knockout mice lacking two of the actin filament disassembly factors exhibit fewer myelin wraps (Nawaz et al., 2015). Taken together, these findings suggest that actin filament depolymerization may provide a driving force for myelin membrane wrapping around axons.

Presumably, oligodendrocytes need to coordinate the delivery of membrane vesicles and modulate actin cytoskeleton dynamics in a site-specific manner. According to the new model

summarized in Fig. 2, the growth rates of various sites among the advancing growth zone need to be differentially regulated as a myelin sheath is being formed. In order for the whole myelin membrane sheet to reach the final trapezoid shape (when unrolled), radial growth must gradually attenuate when the final number of wraps is reached, while the longitudinal growth persists such that the newer and shorter inner layers catch up with the more mature, longer outer layers. However, how this differential regulation is achieved along a continuous inner tongue throughout the formation of a myelin sheath remains unknown.

Once the proper number of wraps is reached around an axon, the radial growth rate of a myelin sheath attenuates. How is this number determined and how does an oligodendrocyte sense that this number of wraps has been achieved? Most myelinated axons tend to have g-ratios (the diameter of the axon divided by the diameter of the axon and its myelin) close to the value optimal for conduction and nervous system efficiency (Chomiak and Hu, 2009), and thicker axons have more wraps (Hildebrand et al., 1993). Intriguingly, the outer and inner tongues of mature CNS myelin are frequently located within the same quadrant in cross sections (Peters, 1964; Waxman and Swadlow, 1976), indicating that oligodendrocytes often make nearly integral numbers of wraps. Remarkably, typical g-ratio values were not observed on myelinated nanofibers (Lee et al., 2012), suggesting the existence of axonal molecular cues that instruct diameter-dependent, and even neuronal activity-dependent, radial growth requirements. Nrg1/ErbB signaling is a good candidate pathway because the manipulation of axonal Nrg1-III levels directly correlates with the total number of wraps produced by Schwann cells (Nave and Salzer, 2006). Although Nrg1/ErbB signaling may play a part in the development of CNS myelin, other surface cues should also exist considering the normal CNS myelination observed in Nrg1 conditional knockout mice (Brinkmann et al., 2008; Mei and Nave, 2014). Signal transduction by these cues may converge on the regulation of membrane vesicle delivery and actin filament turnover to control wrapping. Interestingly, live imaging studies using zebrafish larvae observed

retraction of some myelin sheaths by oligodendrocytes while other myelin sheaths were maintained (Czopka et al., 2013). This raises an important open question: What are the mechanisms underlying myelin retraction? Presumably, the growth zones may also represent collapsing zones of endocytosis and membrane removal. Cytoplasmic channels may then serve as the routes for retrograde trafficking of vesicles out of the myelin sheath. If growth and retraction machinery is differentially adjustable, it is tempting to propose that bidirectional myelin sheath length and radial thickness modulation can be additional mechanisms contributing to circuit-level neural plasticity.

How do the myelin lamellae stack compactly?

Myelin achieves its insulating function by extruding most of the cytoplasm and extracellular space to obtain a low dielectric permittivity, which is vital for lowering axolemmal capacitance. In compact myelin, plasma membranes are brought into extremely close apposition (~1-3 nm) along a large surface area, representing an extraordinary paradigm of membrane remodeling. There are two types of compaction in myelin: compaction between two cytoplasmic membrane leaflets, forming major dense lines under EM, and compaction between two extracellular leaflets, forming intraperiod lines (Figs. 1a,b and 3). It was traditionally thought that the compact myelin components PLP (proteolipid protein) and MBP (myelin basic protein) made up ~80% of CNS myelin proteins and might play vital roles in these compaction processes. While this old view of myelin protein composition appears relatively simple, the mechanisms underlying myelin compaction have been studied for decades and are more complex than originally thought.

MBP is a small cytoplasmic protein which constitutes ~8% of the myelin proteins (Jahn et al., 2009). In shiverer mice, which lack MBP, the few myelin sheaths, if any, frequently lack major dense lines and fail to be compacted (Bird et al., 1978; Privat et al., 1979; Rosenbluth, 1980).

This suggests that MBP participates in compaction between two cytoplasmic membrane leaflets. MBP can bear up to 19 net positive charges at neutral pH and was shown to bind the negatively charged lipid head groups (Harauz et al., 2009; Harauz and Libich, 2009; Nawaz et al., 2009). MBP also contains amphipathic α-helices that can be partly embedded in the membrane leaflet (Harauz et al., 2009; Harauz and Libich, 2009). Therefore, MBP can associate with membranes as a peripheral membrane protein through both electrostatic and hydrophobic interactions. Together with its small size, MBP neutralizes repulsive negative charges on the membranes and can potentially bring two cytoplasmic leaflets into close apposition (Fig. 3). Additionally, upon the interaction of MBP with membranes, it can self-associate into a high-order ensemble (Aggarwal et al., 2013; Aggarwal et al., 2011; Kattnig et al., 2012). While MBP is an overall intrinsically disordered protein, its interaction with membranes induces formation of α-helices and β-sheets (Aggarwal et al., 2011; Harauz et al., 2009). Through charge neutralization by elevating pH in vitro, purified MBP was shown to form micrometer-scale droplets in a reversible way, and this may involve a mechanism similar to amyloid-like β-aggregation (Aggarwal et al., 2013). Accordingly, the idea of phase transition of low-complexity disordered proteins into a hydrogel-like cohesive meshwork has been introduced for MBP. Consistent with the fact that a critical concentration is required for phase transition, recent studies using the surface forces apparatus described a cooperative membrane adsorption of MBP when its concentration exceeds a certain level (Lee et al., 2014). When MBP is deposited between two membranes in heterologous cell lines, in the membrane sheets of cultured oligodendrocytes, or in cell-free membrane systems, proteins with 30 amino acid residues or more on the cytosolic side are excluded from the MBP-occupied domains (Aggarwal et al., 2013; Aggarwal et al., 2011). Assembly of a meshwork by phase transition may be the mechanistic basis of the observed diffusion barrier activity. Altogether, by interaction with membranes, self-assembly into a cohesive network and extrusion of proteins over a certain size, MBP promotes myelin compaction on the cytoplasmic side (Fig. 3).

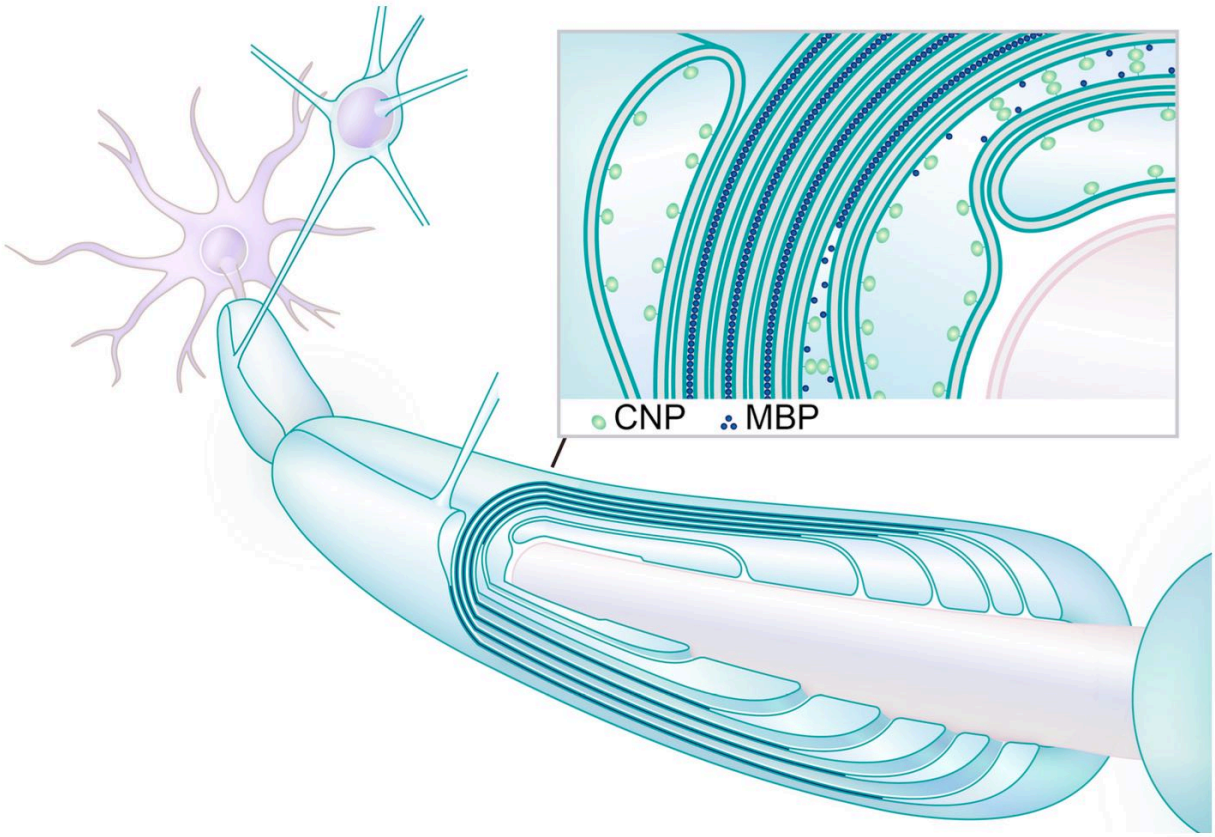

Figure 1-3 | Intracellular compaction of myelin membranes.

The detailed illustration shows an actively forming myelin sheath with six lamellae, where compaction has spread to the fourth outermost layer. Compaction progresses both radially and longitudinally in parallel with membrane growth (cf. Fig. 2). In the longitudinal view, compaction of the middle two layers is still ongoing toward the paranodal loops. Compaction is completed for the two outermost layers and has not started for the two innermost layers. The inset shows a close-up view of an area covering the outer tongue, compacted and non-compacted layers, and the inner tongue. In the region dominated by non-compact myelin components including CNP, the concentration of MBP is relatively low and the membranes are separated by the cytoplasm. After reaching a certain concentration, MBP closely binds two apposed membranes together, and non-compact myelin components and the cytoplasm are extruded; thereby membranes are compacted in a “zippering”-like fashion. The inset was adapted from (Snaidero and Simons, 2014) with permission of The Company of Biologists.

On the extracellular side of the membrane, transmembrane protein PLP exhibits membrane adhesion activities in vitro (Bakhti et al., 2013; Bizzozero and Howard, 2002; Palaniyar et al., 1998). Due to its high abundance in CNS myelin (~17% of total protein (Jahn et al., 2009)), it was assumed to play an important role in compact myelin formation. Surprisingly, PLP-null mice produce nearly normal amounts of myelin (Klugmann et al., 1997). By high-pressure freezing with freeze substitution, PLP-null myelin exhibits no conspicuous intraperiod line defects (Möbius et al., 2008), implying that PLP only plays a minor role in the maximal stability of compact myelin, or that its role is functionally redundant with other molecules. Unfortunately, this leaves the detailed mechanisms crucial for the extracellular membrane compaction in the CNS mostly unclear. It has been proposed that intraperiod line formation may not require specific adhesive molecules but alternatively may be mediated by nonspecific van der Waals interactions and hydrogen bonding between membranes (Bakhti et al., 2013; Coetzee et al., 1999). The major forces opposing extracellular compaction that need to be overcome include electrostatic repulsion and steric hindrance exerted by the glycocalyx on the membrane surface (Bakhti et al., 2013). In this regard, the extracellular compaction may be facilitated by the intracellular compaction as many transmembrane glycoproteins are excluded from the MBP-occupied domain (Aggarwal et al., 2013). However, it should be noted that intraperiod lines are still formed in the shiverer mice (Inoue et al., 1981; Privat et al., 1979), indicating the extracellular compaction can happen independently of intracellular compaction. Interestingly, overexpression of a polysialyltransferase in myelinating oligodendrocytes induces increased surface levels of polysialic acids, which are highly anionic and have a large hydration volume (Bakhti et al., 2013; Schnaar et al., 2014). In these cells, myelin lamellae were split when examined via conventional fixation and EM techniques (Bakhti et al., 2013). Together with the observation of a decrease in the surface sugar residues along oligodendrocyte differentiation, these findings suggest that removal of the glycocalyx via the normal oligodendrocyte

differentiation program may be a prerequisite in order to remove the opposing force against and unmask the weak interactions for the extracellular compaction (Bakhti et al., 2013).

One important aspect that remains unclear is how all the aforementioned findings on the intracellular and extracellular compaction can be fit into the spatiotemporal progression of myelin compaction in vivo. Early EM studies observed that compaction starts before there are more than three myelin layers (Hildebrand et al., 1993). A recent study found that the intraperiod lines can be observed between layers that still contain the cytoplasm during early development (Snaidero et al., 2014). Thus, the differentiation program may downregulate the enzymes and membrane proteins contributing to the glycocalyx and upregulate PLP early before the intracellular compaction, uncovering and enhancing the weak interactions for the extracellular compaction.

The same recent study further demonstrated that the intracellular compaction starts from the outermost layers and extends inward (Figs. 2 and 3) (Snaidero et al., 2014). Intriguingly, the progression of the intracellular compaction is largely affected by the relative amounts of MBP and the most abundant noncompact myelin component CNP (2′,3′-cyclic nucleotide 3′-phosphodiesterase; ~4% of total myelin proteins (Jahn et al., 2009)). Intracellular compaction is more advanced in Cnp+/- mice (Snaidero et al., 2014). On the other hand, in the heterozygous shiverer mice, there is a delay in the intracellular compaction (Snaidero et al., 2014). Moreover, overexpression of CNP inhibits the intracellular compaction; in uncompacted regions, CNP far outnumbers MBP, and vice versa for the compacted regions (Gravel et al., 1996; Yin et al., 1997). These observations imply that the ‘dynamics’ of the intracellular compaction may be governed by the mutual exclusion between MBP and noncompact myelin components including CNP (Fig. 3). This is reminiscent of the intra-axonal boundary resulting from the mutual exclusion of different cytoskeletal scaffold proteins, resulting in the assembly of a distinct

molecular domain at the axon initial segment (Galiano et al., 2012; Normand and Rasband, 2015). Remarkably, the length and location of the axon initial segment can be adjusted due to changes in neuronal activity (Yoshimura and Rasband, 2014). A similar scenario may be also involved in the dynamic CNP/MBP competition that could be utilized to reopen the cytoplasmic channels in mature sheaths in order to change their thickness or even retract them. Therefore, further understanding of CNP/MBP dynamics will be required to elucidate not only the spatiotemporal onset and progression patterns of intracellular compaction during development, but also the potential mechanisms for activity-dependent myelin remodeling.

Our current understanding of the mechanisms regulating compaction is still not sufficient to explain how the cytoplasmic channels are left open during active myelination and later buried when myelin matures. Along the same lines, another open question is how the paranodal loops, inner cytoplasmic collars and outer tongues remain uncompacted (Fig. 2). It is tempting to propose that the cooperative regulation of dynamic molecular competition and membrane apposition may play an important role. Furthermore, the potential for the process of decompaction to participate in myelin retraction and thickness modulation is wholly unexplored. Future studies will be required to address all of these questions.

“Plastic” wrap – Optimization and the call of activity

Myelin is not simply a static structure in place to ensure rapid conduction. In our nervous systems, functional optimization cannot be fulfilled merely by maximizing conduction velocity (Seidl, 2014; Waxman, 1997). One prominent example is the avian auditory system (Seidl et al., 2010). In a specific group of neurons in the chicken auditory brainstem, each axon branches to propagate action potentials to both the ipsilateral and contralateral targets within the brainstem. While the contralateral path is around twice as long as the ipsilateral one, the axon diameter

and myelin sheath lengths of the ipsilateral axon are smaller and shorter, respectively, resulting in a two-fold slower conduction velocity. The overall effect is isochronicity of the conduction time between the two paths, down to sub-millisecond precision. Therefore, not all the myelin sheath parameters are optimized for the fastest action potential conduction. Oligodendrocytes appear to be responsive to individual axons and adjust myelination parameters according to their needs. Such plastic regulation of myelination has been greatly appreciated recently (reviewed in (de Hoz and Simons, 2015; Richardson et al., 2011; Wang and Young, 2014; Zatorre et al., 2012)), but the mechanisms underlying this active regulation of myelination remain poorly understood.

Myelination can modulate information flow in neural circuits by a number of potential mechanisms, including (1) de novo myelination of unmyelinated axons or unmyelinated segments within myelinated axons, (2) myelin replacement, where an old sheath is replaced with a new one, (3) thickening or thinning of existing sheaths, (4) lengthening or shortening of existing sheaths, and (5) myelin retraction, where sheaths are removed and are not replaced. Each step of myelination, from target selection and wrapping to myelin compaction during sheath maturation could be coordinately regulated to mediate these processes and achieve a functional change in a neural circuit. An interesting future challenge will be to determine whether these mechanisms of myelin-based neural plasticity are actually utilized in vivo, and if so, under what conditions.

There is emerging and strengthening evidence that myelin-based mechanisms of neural circuit regulation are active in the mouse brain. During development, many unmyelinated axons or unmyelinated segments of axons are present while normal developmental myelination is ongoing. A recent study illustrates that juvenile social isolation (for two weeks after the mice are weaned) leads to thinner and fewer myelin sheaths made by individual oligodendrocytes specifically in the medial prefrontal cortex (Makinodan et al., 2012). The affected mice exhibit

defective sociability and working memory. These results suggest that myelination by oligodendrocytes can be adjusted by their microenvironment, probably shaped by neuronal activity resulting from the external stimuli experienced by the organism. Complementing these findings, another study deprived adult mice of social interaction for eight weeks and observed thinner myelin and decreased myelin gene expression specifically in the prefrontal cortex (Liu et al., 2012). Remarkably, four weeks of social re-integration restored myelin gene expression and reversed behavioral deficits. The recovery after social re-integration might result from the thickening of the thinner myelin sheaths or resumed wrapping processes. The surprising effects of social isolation on myelination patterns and behavior in both adolescence and adulthood beg the question: what is the potential for myelin remodeling in the adult CNS?

In the adult CNS, oligodendrocyte precursor cells are broadly distributed and serve as a source of adult-born myelinating oligodendrocytes (de Hoz and Simons, 2015; Richardson et al., 2011; Wang and Young, 2014; Zatorre et al., 2012). Early EM studies observed many unmyelinated axons of 0.4-0.8 μm in diameter in the CNS (Hildebrand et al., 1993) and the recent study reconstructing large EM data sets even revealed long unmyelinated sections of otherwise myelinated axons in the adult cortex (Tomassy et al., 2014). These findings suggest that unmyelinated and incompletely-myelinated axons could be putative substrates for de novo myelination in the adult brain. Considering the findings that newly formed oligodendrocytes generate myelin sheaths only within a short time (Czopka et al., 2013; Watkins et al., 2008), generation of new myelin sheaths in adulthood may require the generation of new oligodendrocytes. Consistently, by tracing the 14C concentration in purified oligodendrocyte DNA from postmortem human brains combined with mathematical modeling, the population of oligodendrocytes in the cortex was estimated to expand until the end of the fourth decade of age and have an annual turnover rate of 2.5% afterwards (Yeung et al., 2014). Furthermore, another recent study showed that learning to run on a complex wheel with irregular rung

spacing enhanced the proliferation of oligodendrocyte precursor cells and increased the number of newly formed oligodendrocytes in adult mice (McKenzie et al., 2014). When the generation of new myelin-forming oligodendrocytes was genetically abolished in adult mice, they performed worse in mastering the complex wheel running than the control mice (McKenzie et al., 2014). These results imply that adult myelination by newly formed oligodendrocytes plays an important role in motor learning.

The findings in development and adulthood are consistent with the idea that the environmental stimuli increase neuronal activity, which in turn stimulates oligodendrogenesis and myelination. A role for activity in modulating myelination has been proposed for decades (Fields, 2008). Several studies have directly tested this role in vivo. For example, one study showed that unilateral stimulation of the rat corticospinal tract selectively induces proliferation and differentiation of oligodendrocyte precursor cells on the stimulated side (Li et al., 2010). Another recent study utilized channelrhodopsin to increase neuronal firing activity in the mouse M2 motor cortex. The authors observed increased oligodendrogenesis as well as thicker myelin sheaths in the area near the stimulated neurons and their axons (Gibson et al., 2014).

Taken together, the social isolation and directed neural stimulation studies suggest that myelin segment thickness can be modulated by neuronal activity. The particular mechanisms translating environmental experience into oligodendrocyte regulation of myelin thickness remains poorly understood. In these particular studies, whether thinner or thicker myelin observed represents remodeled or de novo myelination remains unclear. However, increasing the thickness of existing myelin sheaths has been proven feasible. The inducible conditional knockout of Pten (phosphatase and tensin homolog) in mature oligodendrocytes of adult mice was reported to make the myelin dramatically thicker by reopening the cytoplasmic channels in the myelin sheaths, resulting in more wrapping (Goebbels et al., 2010; Snaidero et al., 2014).

By contrast, much less is known about thinning of existent myelin sheaths. However, myelin sheath retraction has been observed in live imaging of developing zebrafish larvae (Czopka et al., 2013). Myelin thinning may be achieved by modulating the same machinery used in myelin retraction.

Myelin retraction observed during zebrafish development unexpectedly reveals some uncertainty of target selection by oligodendrocytes in vivo. It suggests that dynamic regulation may be involved in editing the decision made during initial contact and target selection. It is currently unclear how an oligodendrocyte selects and stably myelinates only a subset of biophysically suitable substrates in the local environment. Two recent studies provide compelling evidence that this process may not require but is partially affected by neuronal activity (Hines et al., 2015; Mensch et al., 2015). When neurons in zebrafish larvae express tetanus neurotoxin to inhibit synaptic vesicle release, individual oligodendrocytes form fewer myelin sheaths (Hines et al., 2015; Mensch et al., 2015). Though differences in study design seemed to lead to different mechanistic interpretations, this deficit is likely due to decreased nascent sheath stability. It appears that more of the ensheathments on silent axons may be ≤ 5 μm long and sustained for ≤ 10 minutes, and there may be more sheaths on silent axons that are stable for 6 hours but retract afterwards. Therefore, neuronal activity may modulate myelination by influencing the stable growth and subsequent maintenance of nascent myelin sheaths. Interestingly, oligodendrocyte precursor cells form synapses with axons and express neurotransmitter receptors. These synapses directly connect neurons with oligodendrocyte precursor cells in all grey and white matter areas explored so far and allow oligodendrocyte precursor cells to sense most aspects of neuronal activity (Bergles et al., 2000; Kukley et al., 2007; Lin and Bergles, 2004; Ziskin et al., 2007). The physiological role of the neuron-glial synapses and how oligodendroglia respond to neuronal activity by modulating myelination in vivo are currently under vigorous investigation.

In the emerging field of myelin plasticity, several key challenges await to be addressed to understand its role in modulating neural plasticity and circuit-level activity patterns. First, whether activity- or experience-dependent changes in myelination patterns are a specific or general phenomenon must be addressed. Directly linking changes in a neuron's activity with its own altered myelination profile, while technically challenging, would provide extremely compelling support of specificity. Secondly, identifying neuronal and glial molecular regulators of myelination underlying how oligodendroglia respond to neuronal activity in vivo has been of long-standing interest in the field of myelination, which only continues to grow as myelin's role in affecting neural function increases. Finally, demonstrating that changes in myelination patterns of specific circuits have functional behavioral consequences will go far in cementing myelin's role as a major, potentially bidirectional regulator of neural function and plasticity. While this experimental wish list may be currently addressable in part, full illumination of its answers awaits the future development of tools and techniques able to overcome current limitations in spatiotemporal resolution.

Since its discovery over 160 years ago (Virchow, 1854), the study of myelin has endured despite its simplistic reputation as a passive sidekick insulator of axons, with oligodendroglia being once overlooked among the non-neuronal, non-glial "third element" of the nervous system (Pérez-Cerdá et al., 2015). Now, oligodendrocyte myelination is starting to reveal itself as the dark horse in the race to understand the subtle and sophisticated inner-workings of the nervous system. If restrictive stereotypes of myelin's potential can be released and this enigmatic structure given the respect it now so clearly deserves, only time will tell how fast and how far it will carry our understanding of the brain.

Chapter Two: Somatodendritic Expression of JAM2 Inhibits Oligodendrocyte Myelination

Abstract

Myelination occurs selectively around neuronal axons to increase the efficiency and velocity of action potentials. While oligodendrocytes are capable of myelinating permissive structures in the absence of molecular cues, structurally permissive neuronal somata and dendrites remain unmyelinated. Utilizing a purified spinal cord neuron-oligodendrocyte myelinating coculture system, we demonstrate that disruption of dynamic neuron-oligodendrocyte signaling by chemical crosslinking results in aberrant myelination of the somatodendritic compartment of neurons. We hypothesize that an inhibitory somatodendritic cue is necessary to prevent non-axonal myelination. Using next-generation sequencing and candidate profiling, we identify neuronal Junction Adhesion Molecule 2 (JAM2) as an inhibitory myelin-guidance molecule. Taken together, our results demonstrate that the somatodendritic compartment directly inhibits myelination, and suggest a model in which broadly indiscriminate myelination is tailored by inhibitory signaling to meet local myelination requirements.

Introduction

The central nervous system (CNS) greatly benefits from oligodendrocyte myelination. Myelin supports the clustering of ion channels to nodes of Ranvier and increases the resistance across the axonal membrane. These properties generate the saltatory conduction of action potentials, ensuring rapid and efficient neural communication over longer distances in a more compact space (Zalc et al., 2008). It has long been appreciated that myelin, with very few exceptions, forms selectively around axons (Braak et al., 1977; Lubetzki et al., 1993; Blinzinger et al., 1972; Remahl and Hildebrand, 1985; Cooper and Beal, 1977). This begs the fundamental question: how does an oligodendrocyte, the myelin-forming cells of the CNS, target each of its many myelin segments exclusively to axons?

Very little is currently known about axon selection by oligodendrocytes. More well understood are the consequences of when myelin fails to form correctly around axons, such as in leukodystrophies, or when myelin is attacked by the immune system, as in multiple sclerosis. In such cases, neuronal function is impaired and neurons eventually degenerate if myelin is not reformed (Fancy et al., 2011; Franklin and ffrench-Constant, 2008; Trapp and Nave, 2008; Yuen et al., 2014). In development, the coordinated differentiation and myelination of thousands of spatially distributed oligodendroglia is thought to be extrinsically determined, perhaps by neuronal activity. Indeed, recent findings suggest that neuronal activity is involved in modulating axon selection and the extent of myelin segment formation (Gibson, 2014; Hines et al., 2015; Mensch et al., 2015).

An unexplored aspect of myelination is the avoidance of selecting non-axonal targets. In CNS gray matter, oligodendrocytes must select axons while avoiding neuronal cell bodies, dendrites and processes of other glial cells. How is this specificity accomplished? Little evidence of non-

axonal oligodendrocyte myelination exists (Blinzinger et al., 1972; Braak et al., 1977). Curiously, *in vitro*, oligodendrocyte myelination is not limited to axons: oligodendrocytes produce myelin membranes on planar glass coverslips, cylindrical polystyrene nanofibers (Bechler et al., 2015; Lee et al., 2012), and conical glass micropillars (Mei et al., 2014). These observations suggest that myelin substrate selection is not cell-intrinsically limited to physiologically relevant axon-like geometries, and that an inductive cue is not strictly required for differentiation and myelination. Oligodendrocyte cell processes are thus likely sensitive to cell-extrinsic 'myelin guidance' cues that ensure only correct selection of pre-myelinated axons.

We propose three potential mechanisms that would ensure correct axonal selection (Fig 1a). An attractive signal may be expressed by the neuronal axon (Fig 1a, 'Attraction') to specifically promote myelin formation. Alternatively, proper myelination of axons may be achieved by expression of an inhibitory cue by the neuron's somatodendritic compartment (Fig 1a, 'Inhibition'). Here, oligodendrocyte processes form myelin segments around permissive axons but not on inhibitor-expressing structures. However, the Attraction and Inhibition models are not mutually exclusive, and both modes of signaling may be at play to ensure proper targeting of myelin segments (Fig 1a, 'Mixed'). Which of these signaling mechanisms are active during developmental myelination? By utilizing a purified spinal cord neuron-oligodendrocyte myelinating coculture system, we demonstrate that disruption of dynamic neuron-oligodendrocyte signaling results in aberrant myelination of the somatodendritic compartment of neurons indicative of an active inhibitory mechanism. Using next-generation sequencing and candidate profiling, we identify Junction Adhesion Molecule 2 (JAM2) as a somatodendritic protein necessary and sufficient to inhibit oligodendrocyte myelination. Taken together, our results demonstrate that the somatodendritic compartment directly inhibits myelination, and provide a model in which broadly indiscriminate myelination is tailored by inhibitory signaling to meet local myelination requirements.

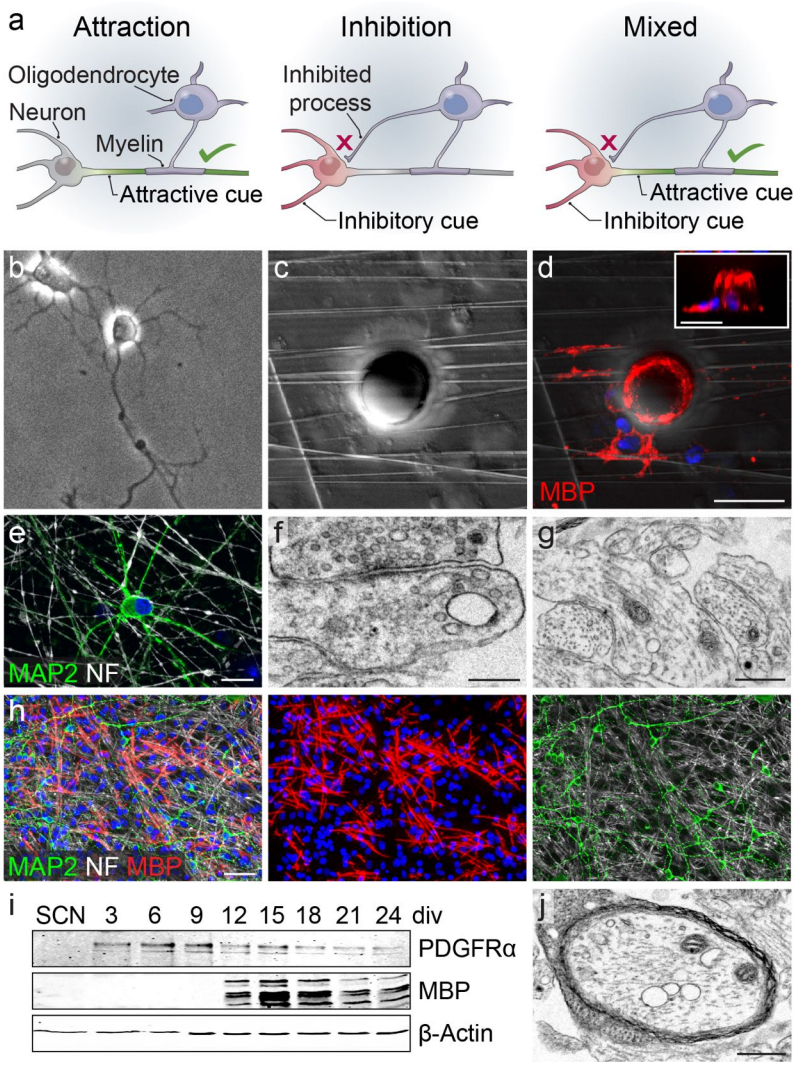

Figure 2-1 | Myelin target selection by oligodendroglia.

(a) Models of oligodendrocyte axon selection and myelination. Attraction: an attractive cue is expressed on the axon (green), resulting in its myelination by the oligodendrocyte, while no myelination cues are present on non-myelinated structures (gray). Inhibition: non-myelinated structures express an inhibitory cue (red), resulting in oligodendrocyte process inhibition and myelination of inhibition-free axons (gray). Mixed: Inhibitory (red) and attractive (green) cues result in the correct myelination of axons. (b) a phase image of a spinal cord neuron (SCN) in culture. (c) a phase image of nanofibers and a 20-micrometer diameter polystyrene bead. (d) an oligodendrocyte ensheathing myelin basic protein-positive (MBP+, red) membranes on nanofibers and the bead shown in (c) with a side-view shown in the inset. (e) a neuron at eight days in vitro immunostained for microtubule associated protein 2 (MAP2) and neurofilament (NF). (f) electron micrograph of a synapse, and (g) neurofilament-positive axons in SCN cultures. (h) low-magnification image of neurons and oligodendroglia in a myelinating coculture. (i) timecourse of oligodendrocyte progenitor cell (OPC) and oligodendrocyte protein expression in SCN myelinating cocultures. (j) electron micrograph of a myelinated axon in a myelinating spinal cord neuron coculture. Scale bars = 20 micrometers (d), 10 micrometers (e), 250 nanometers (f), 500 nanometers (g, i), 50 micrometers (h).

Results

The somatodendritic compartment is biophysically permissive to myelin ensheathment

To understand the nature of selectivity and fidelity of the myelination process, we reasoned that the presence of a somatodendritic inhibitor would only be required if oligodendrocytes are capable of ensheathing the spherical shape of a neuron cell body (Fig 1b). To test this possibility, we cultured primary rat oligodendrocyte precursor cells (OPCs) on nanofibers with 20-micrometer diameter polystyrene beads that mimic neuron cell body geometry (Fig 1c). We find that differentiated myelin basic protein-positive (MBP+) oligodendrocytes readily ensheathe myelin membranes around both nanofibers and beads (Fig 1d).

We then asked whether the somatodendritic compartment remains unmyelinated due to lack of attraction, or expression of inhibition? To investigate this question, we developed a primary purified spinal cord neuron (SCN) and oligodendroglial myelinating coculture system (Fig 1b,e-i). The SCN cultures robustly exhibited extensive axons, dendrites, and formed neuronal synapses over the course of three weeks *in vitro* (Fig 1e-g). Under normal conditions, purified OPCs seeded onto mature SCN cultures proliferate, differentiate after approximately one week *in vitro* (Fig 1h-i), and form compact layers of myelin membrane around axons (Fig 1j). Oligodendrocytes wrap myelin membrane around axons while avoiding neuron somata and dendrites (Fig 2a) (Lubetzki et al., 1993), recapitulating gray matter myelination patterns *in vitro*. We then asked whether dynamic neuron-oligodendrocyte signaling is required to prevent myelination of the somatodendritic compartment. Prior to seeding neuron cultures with OPCs, we treated the neurons with the chemical cross-linker paraformaldehyde (PFA) (Rosenberg et al., 2008). Surprisingly, oligodendrocytes wrapped myelin membranes on fixed neuron somata and dendrites in addition to axons (Fig 2b-c), and form multiple compacted layers of myelin membrane around cellular processes (Fig 2d-e). It is important to note, that paraformaldehyde

cross-linking and the extended period of coculturing, subcellular structures are not well maintained (Rosenberg et al., 2008), making it impossible to determine whether myelinated structures are axons or dendrites. Based on our observations that (1) cultured oligodendroglia ensheathe bare nanofibers and microbeads, (2) avoid ensheathing neural somatodendritic compartments *in vitro* and *in vivo*, yet (3) aberrantly ensheathe cross-linked somata and dendrites, we hypothesize that neurons must express inhibitory molecules to prevent somatodendritic myelination.

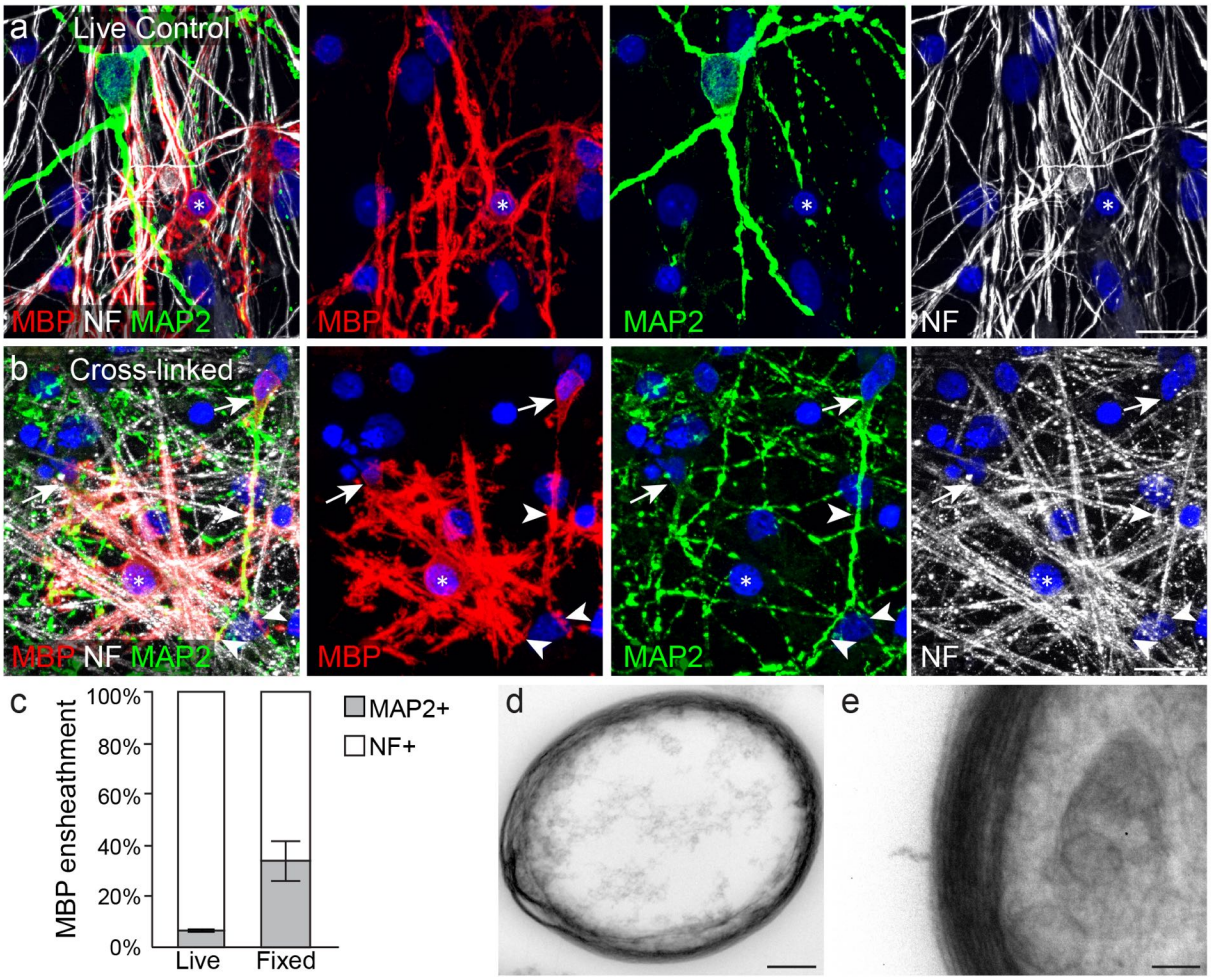

Figure 2-2 | Oligodendrocytes wrap somatodendritic compartments of chemically cross-linked neurons.

(a) an oligodendrocyte (asterisk) forms MBP+ myelin segments on SCN axons (NF, white) but not dendrites (MAP2, green). (b) an oligodendrocyte (asterisk) forms myelin segments on paraformaldehyde cross-linked SCN axons, dendrites (arrowheads), and somata (arrows). (c) quantification of MBP+ ensheathments on either MAP2+ dendrites or NF+ axons in live and cross-linked ('Fixed') cocultures. (d-e) multiple layers of myelin membrane formed in a cross-linked myelinating coculture. DAPI, blue. Bar graph in (c) represents means with s.e.m. error bars. n = 4 experiments quantified from 26-30 20x fields per condition per experiment. Significance was calculated using one-tailed paired Students t-test. P = 0.04. Scale bars = 20 micrometers (a,b), 500 nanometers (d), 100 nanometers (e).

Differential RNA-seq and candidate profiling for myelination-inhibitory molecules

To identify candidate inhibitory molecules, we conducted next-generation RNA-sequencing of SCN as well as dorsal root ganglion neuron (DRG) cultures (Fig 3a). We reasoned that differential expression analysis would increase the likelihood of identifying a somatodendritic inhibitor of myelination because SCN cultures develop extensive dendritic arbors around their somata, while pseudo-unipolar DRG neurons lack true dendrites. Candidate inhibitory proteins were chosen based on the following criteria: proteins that have (1) significantly higher expression in SCNs as compared to DRGs, and (2) transmembrane domains (Fig 3b). The differential RNA-seq analysis yielded two distinct populations of transcripts, representing higher expression in either DRGs (Fig 3b-d, black) or SCNs (Fig 3b-d, dark gray/pink). Several genes that have been described in the literature as expressed in either DRGs or SCNs were also differentially expressed in our analysis (Fig 3d, black and gray bars). Overall, 170 unique genes were identified as candidate inhibitory proteins (Fig 3b-d, pink). By profiling and prioritizing candidates from the RNAseq analysis, we identified the protein Junction Adhesion Molecule 2 (JAM2) as a differentially expressed (Fig 3d-e) potential inhibitor of myelination because of its low expression in DRG somata (Fig 3f, insert), little to no expression in the majority of DRG (Fig 3f) and SCN axons (Fig 3g), and its high expression and specific localization on the somatodendritic compartment of SCN (Fig 3g).

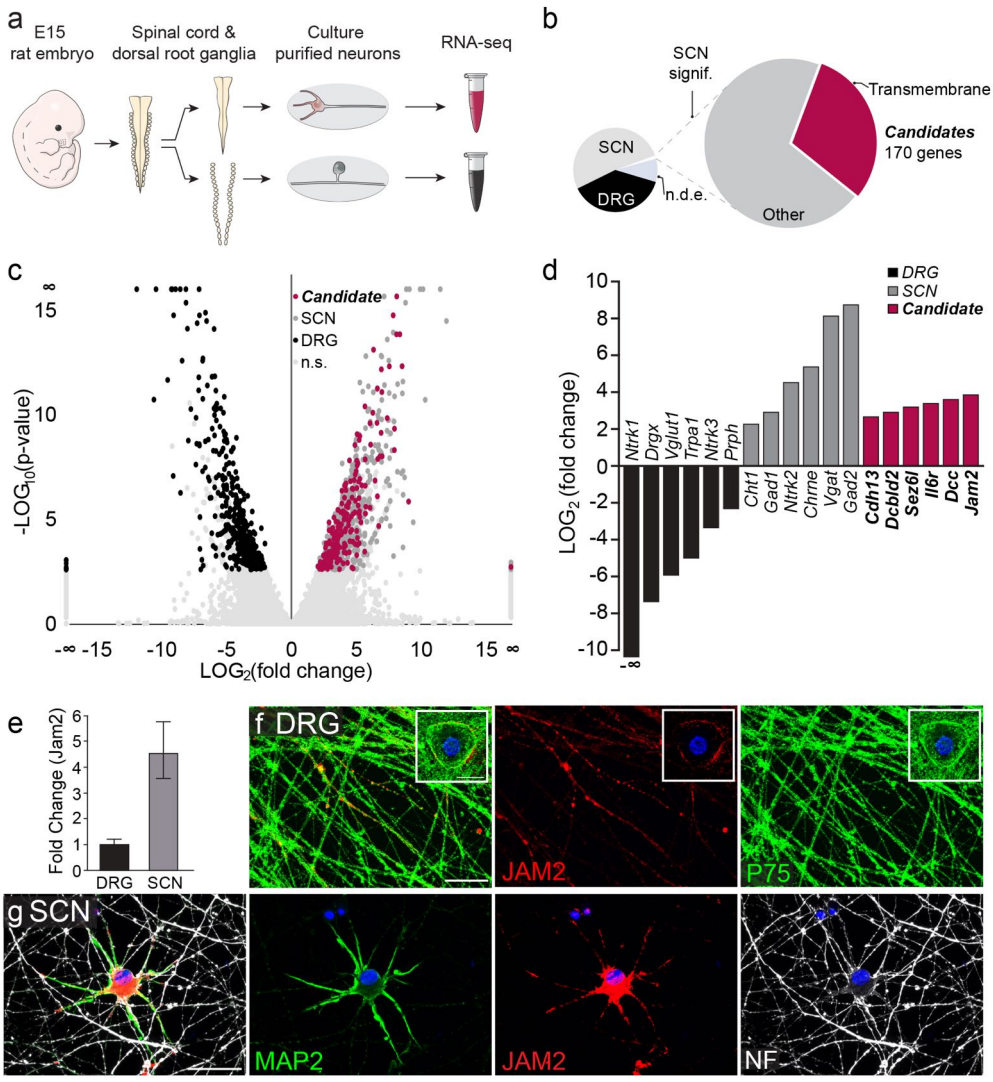

Figure 2-3 | Differential RNA-Seq and candidate profiling.

(a) Experimental procedure for RNA extraction. Embryonic day 15 (E15) rat embryos were dissected and their spinal cords and dorsal root ganglia were isolated. SCN and dorsal root ganglion neurons (DRG) were separately cultured and their RNA was collected for sequencing (RNA-seq). (b) Results of differential RNA-seq. Candidate inhibitory proteins are SCN transcripts that are significantly differentially expressed (large pie chart, right), are localized to the plasma membrane and have transmembrane domains (pink). Transcripts detected also included other SCN transcripts (big pie chart, light gray), SCN enriched, but not significantly differentially expressed (small pie chart, gray), DRG-enriched transcripts (black) and not differentially expressed transcripts (n.d.e.). (c) Volcano plot of DRG (black) and SCN (dark gray), SCN candidate ("Candidate", pink), and not significantly differentially expressed ("n.s.", light gray) transcripts. (d) Examples of differentially expressed transcripts from (c). (e) qPCR amplification of jam2 from cultured DRG and SCN, normalized to DRG expression. (f) DRG somata and axons (P75, green) immunostained for JAM2 (red), and (g) Cultured SCN somatodendritic compartment (MAP2, green) and axons (NF, white), and DAPI, blue. Bar graph in (e) represents mean and s.e.m. from n = 4 biological replicates. Gapdh was used as an internal control. Scale bars = 20 micrometers.

JAM2 is sufficient to inhibit oligodendroglial wrapping

JAM2 is a single-pass transmembrane protein with two extracellular immunoglobulin-like domains (Arcangeli et al., 2013). We found that the extracellular portion of JAM2 fused to the Fc region of immunoglobulins ('JAM2-Fc') strongly binds to MBP-positive oligodendrocytes and weakly to PDGF receptor alpha-positive (PDGFRα+) OPCs (Fig 4a) compared to an Fc only negative control (Fig 4b). This suggests that oligodendroglia express at least one JAM2 receptor, and the expression of JAM2 receptor(s) is upregulated as oligodendroglia differentiate. We hypothesized that if JAM2 acts to inhibit myelination, oligodendrocytes will avoid wrapping JAM2-coated permissive structures *in vitro.* To test this possibility, we adapted the micropillar array platform (Mei et al., 2014) (Fig 4c) to assay the activity of Fc-fusion proteins on oligodendroglial wrapping. Wildtype OPCs were seeded onto micropillars coated with either JAM2-Fc or Fc alone. Under control conditions, OPCs and oligodendrocytes associate with micropillars and wrap them with PDGFRα+ or MBP+ membranes. When a single optical section is taken through the micropillar array, immunostained OPC and oligodendrocyte wrapping is visualized as a ring (Figure 4d). Compared to Fc alone, oligodendrocytes wrap significantly fewer JAM2-Fc coated micropillars (Fig 4e-h, 85.7% reduction). Interestingly, even OPC wrapping of micropillars is significantly reduced in the JAM2-Fc condition compared with Fc alone (Fig 4h; 66.6% reduction). We reasoned that we might observe a decrease in OPC and oligodendrocyte wrapping if oligodendroglia failed to adhere or differentiate on JAM2-Fc coated surfaces. Due to technical limitations of imaging cells within the micropillar fields, we quantified the densities of OPCs and oligodendrocytes on JAM2-Fc or Fc coated areas directly adjacent to the micropillar arrays. We found no significant difference between the densities of OPCs or oligodendrocytes between JAM2-Fc and Fc conditions (Fig 4i). Taken together, these results show that the extracellular portion of JAM2 is sufficient to specifically inhibit oligodendroglial wrapping without affecting cell density or oligodendrocyte differentiation.

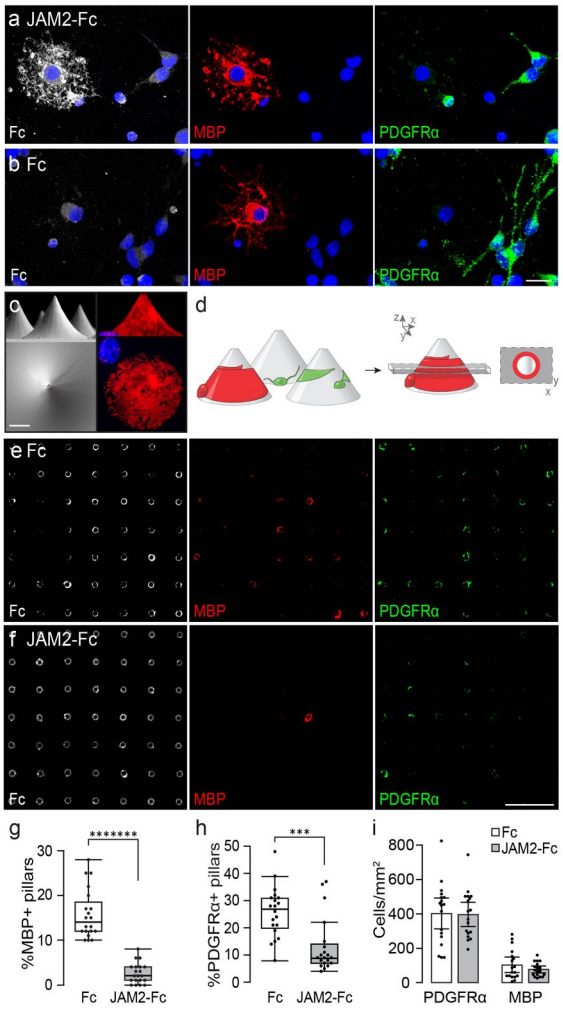

Figure 2-4 | JAM2 is sufficient to inhibit oligodendrocyte wrapping.

(a) JAM2-Fc or (b) Fc protein (white) was cultured with MBP+ oligodendrocytes (red) and PDGFRα+ OPCs (green) to demonstrate JAM2-Fc binding. (c) scanning electron micrograph micropillar array platform (left column) and immunostaining of a cultured oligodendrocyte wrapping a micropillar (MBP, right column) from the x-z plane/side view (top row) and x-y plane/top-down view (bottom row). (d) experimental setup: oligodendroglia are cultured on coated micropillars (left). Myelin membrane (red) wraps of differentiated oligodendrocytes are visualized as rings by taking an optical section (dashed gray box) through immunostained cultures (red ring in x-y plane, far right). Optical sections of (e) Fc- and (f) JAM2-Fc-coated micropillars immunostained for oligodendrocyte (MBP, red) and OPC (PDGFRα, green) wrapping, and micropillars (Fc protein, white). (g) The percentage of micropillars with a MBP+ or (h) PDGFRα+ ring, and the (i) densities of oligodendoglia on flat areas adjacent to micropillars. Box plots (g,h) are defined by the center median line, 25th and 75th percentiles determined by R software, whiskers extend 1.5 times the interquartile range from the 25th and 75th percentiles, and dots outside of whiskers are defined as outliers. n = 20 fields of 100 micropillars (dots) each condition pooled from four independent experiments. Significance was calculated using Wilcoxon Rank-Sum test. (g) *******, P = 6.3x10^{-8}; (h) ***, P = 3.75x10^{-4}. Bar graphs in (i) represent means with s.e.m. error bars. n = 18 10x fields (dots) each condition pooled from three independent experiments. Significance was calculated using two-tailed Students t-test. Scale bars: (a-c) 10 micrometers, (e-f) 400 micrometers.

JAM2 is necessary to prevent somatodendritic myelin wrapping

Given that oligodendrocytes wrap nanofibers, beads, and Fc coated micropillars, but significantly fewer JAM2-Fc coated micropillars, we next asked whether JAM2 signaling is sufficient to inhibit myelin segment formation *in vitro*. We established myelinating SCN cocultures in the presence of either soluble Fc or JAM2-Fc. After seven days, the cocultures were immunostained for MBP and Fc, and the number of MBP+ segments per oligodendrocyte was analyzed. Consistent with Fc binding analysis, myelinating oligodendrocytes in the control condition do not show specific Fc labeling (Fig 5a), while oligodendrocytes in the JAM2-Fc condition show co-labeling of MBP and JAM2-Fc (Fig 5b), indicating that myelinating oligodendrocytes express a JAM2 receptor. Interestingly, we find that the number MBP+ segments formed per oligodendrocyte is significantly reduced in the presence of JAM2-Fc as compared to Fc alone (Fig 5c, 24.6% reduction).

Next, we investigated whether JAM2 is necessary to prevent somatodendritic myelin wrapping of SCNs. First, we established myelinating cocultures with wildtype SCN and OPCs, and allowed them to interact normally for five days *in vitro*. During the final two days of coculture, at the onset of OPC differentiation and initiation of myelination, we applied a function-blocking antibody against JAM2 (Fig S1a-c). In control conditions, oligodendrocyte segments are overwhelmingly wrapped on axons (Fig S1a). However, in the presence of JAM2 function-blocking antibody, we found that oligodendrocytes wrap significantly more MBP+ segments on neuronal dendrites (Fig S1b-c, 321.8% increase).

To understand whether neuronal JAM2 is necessary to ensure that the somatodendritic compartment remains unmyelinated, we established myelinating cocultures with wildtype OPCs and either JAM2-knockout (JAM2 KO) or wildtype (WT) SCNs. We observed that compared to wildtype SCN controls (Fig 5d), wildtype oligodendrocytes wrapped significantly more MBP+

segments on JAM2-deficient somatodendritic compartments (Fig 5e-f, 226.4% increase). Strikingly, we frequently observed large spheroidal ‘bubbles’ of MBP+ membranes in JAM2 KO neuron cocultures (Fig 5e, MBP panel arrowheads). These structures stood out against the typically cylindrical myelin segments on axons and colocalized with neuronal somata (Fig 5e, MAP2 panel arrowheads). We quantified the relative frequency in which neuron cell bodies are wrapped with myelin membranes, and find that JAM2-knockout somata are five-fold more likely to be wrapped by oligodendrocytes compared with wildtype controls (Fig 5g).

During normal axonal myelination, oligodendrocyte adhesion proteins cause the clustering of neuronal proteins and ion channels to nodes of Ranvier, enabling saltatory conduction of action potentials. We next asked whether aberrant somatic wrapping could affect the molecular organization of JAM2-knockout neurons? Unexpectedly, we observe that MBP+ membrane wrapping of neuronal somata induced the clustering of neuronal contactin-associated protein (CASPR) (Fig S2a, inset 1). Wrapped neuronal dendrites also exhibited clustered CASPR (Fig S2a, inset 2), but unwrapped somata and dendrites showed no CASPR clusters (Fig S2a, inset 3). This pattern of molecular organization is indicative of a direct neuroglial molecular interaction normally restricted to paranodes at the node of Ranvier (Einheber et al., 1997; Eisenbach et al., 2009; Pedraza et al., 2009).

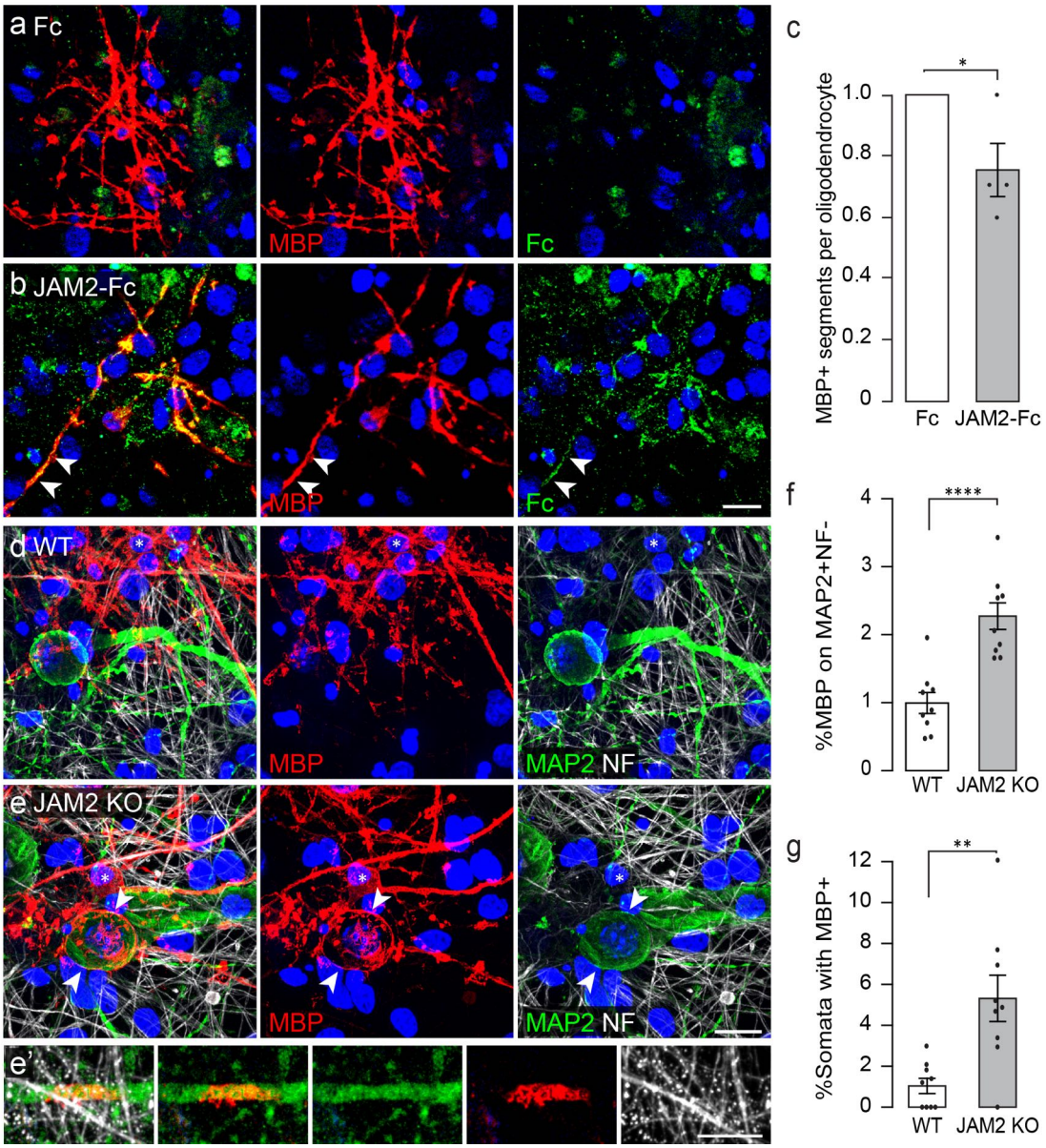

Figure 2-5 | JAM2 is sufficient to reduce myelin segment formation and is necessary to prevent somatodendritic wrapping in vitro.

Oligodendrocytes in SCN cocultures form myelin segments in the presence of soluble (a) Fc or (b) JAM2-Fc protein. (c) the relative number of MBP+ segments formed in the presence of Fc or JAM2-Fc. (d) wildtype or (e) JAM2 KO neurons cocultured with wildtype OPCs for seven days in vitro. Arrowheads indicate myelin membranes on neuron soma and asterisks mark oligodendrocyte cell bodies. (f) the percentage of myelin membrane structures colocalized with MAP2+ and NF- somatodendritic compartments. (g) the percentage of neuron somata wrapped with MBP+ myelin membranes. Bar graphs represent means with s.e.m. error bars. (c) n = 4 independent experiments (dots) representing median number of MBP+ segments formed per oligodendrocyte from 59-79 oligodendrocytes quantified per experiment per condition. (f-g) n = 9 coverslips (dots) pooled from three independent experiments. Significance was calculated using one-tailed paired (c) or unpaired (f-g) Students t-test. (c) *, P = 0.032; (f) ****, P = 7.1x10-5; (g) **, P = 0.0012. DAPI, blue. Scale bars: 20 micrometers.

Loss of JAM2 results in myelination of the somatodendritic compartment *in vivo*

In the more complex environment of the CNS, is inhibitory JAM2 signaling required to prevent myelination of the somatodendritic compartment? At postnatal day 30-31 (P30-31) in the mouse, most neurons in the cervical spinal cord express JAM2. We examined a JAM2 reporter and JAM2 protein expression in spinal cord cross-sections of both *jam2*:beta-galactosidase knock-in mice (Fig S3a-b), as well as heterozygous and JAM2 KO mice, respectively (Fig S3c-d, Fig S4a-b;). The CNS is heavily myelinated and individual myelin segments are generally difficult to resolve by immunostaining. One exception to this technical limitation is the dorsal horn, where very few axons are myelinated. In this area, we observed many beta-galactosidase/NeuN-positive neurons (Fig S3a), and robust gray matter JAM2 immunostaining in heterozygous but not JAM2 KO mice (Fig S4a-b), confirming the specificity of the antibody staining. In P31 littermate wildtype and JAM2 KO mice, we found no significant differences in the average densities of NeuN-positive neurons or CC1-positive oligodendrocytes within the dorsal horn region (Fig S3c-f), suggesting that the development of these two cell types is normal in the absence of JAM2.

When we examined myelination patterns in dorsal horns of littermate wildtype and JAM2 KO mice (Fig 6a-d), we observed conspicuous MBP+ membrane ‘bubbles’ around neuronal somata in JAM2 KO dorsal horns (Fig 6c-d, arrowheads). Seventy-two percent of JAM2 KO hemisections contained more than one myelin-wrapped neuron, compared to just 16% of wildtype hemisections (Fig 6e). Overall, the median number of wrapped neurons per hemisection was four-fold higher in JAM2 KO mice compared to wildtype littermates (Figure 6f). Optical sectioning of immunostained tissue revealed that wrapped neurons could be wrapped with MBP-positive membrane around their entire circumference through several micrometers in

the z-axis (Fig 6g), reminiscent of myelin-wrapped beads (Fig 1d). One of the hallmarks of myelination is the clustering of CASPR to paranodes. Like myelin-wrapped JAM2 KO neurons *in vitro* (Fig S2a), we find that the molecular organization of CASPR on JAM2 KO neurons is dramatically affected by somatic myelination *in vivo.* CASPR protein clustering is evident on MBP+ membrane-wrapped JAM2-knockout neurons (Fig S2b). Consistent with our immunostaining observations, semi-thin sections through a JAM2 KO dorsal horn neuron show myelination around the total circumference of a soma (Fig 6h). This particular cell is wrapped across three different semi-thin sections (Fig S2c-e).

We wanted to further understand the identity of the wrapped Jam2-knockout neurons. Based on our observations that Jam2-knockout neurons are generally wrapped around their entire circumference *in vivo*, are small (10-20 micrometer diameter) and have little cytoplasm (Fig 6c,d,g-h; Fig S2b-c), we screened dorsal horn interneuron markers, and found that MBP+ wrapped neurons are exclusively positive for the paired box gene 2 (PAX2) transcription factor (Figure 7a-e). PAX2+ dorsal horn neurons are inhibitory interneurons and their dendrites and axons exhibit islet morphology oriented along the rostral-caudal axis of the spinal cord (Smith et al., 2015). We find that approximately six-percent of PAX2+ neurons are wrapped in JAM2-knockout mice, significantly more than the under two-percent observed in JAM2-heterozygous mice (Fig 7f). We find no difference in the density of PAX2+ neurons in the dorsal horn between genotypes (Fig 7g). Finally, we find that PAX2+ neurons receive very little presynaptic innervation of their somata (Fig S5a-b) with many cells of both genotypes exhibiting no presynaptic puncta (VGLUT1: 64.4%; VGLUT2: 23.3%; VGAT: 30.6%). We also never observed synaptic puncta between the wrapping MBP+ sheath and the PAX2+ neuron cell body (Fig S5c, 0/480 PAX2+ neurons). Taken together, our observations support the conclusion that oligodendrocyte myelin membranes are in direct contact with neural somata as they wrap.

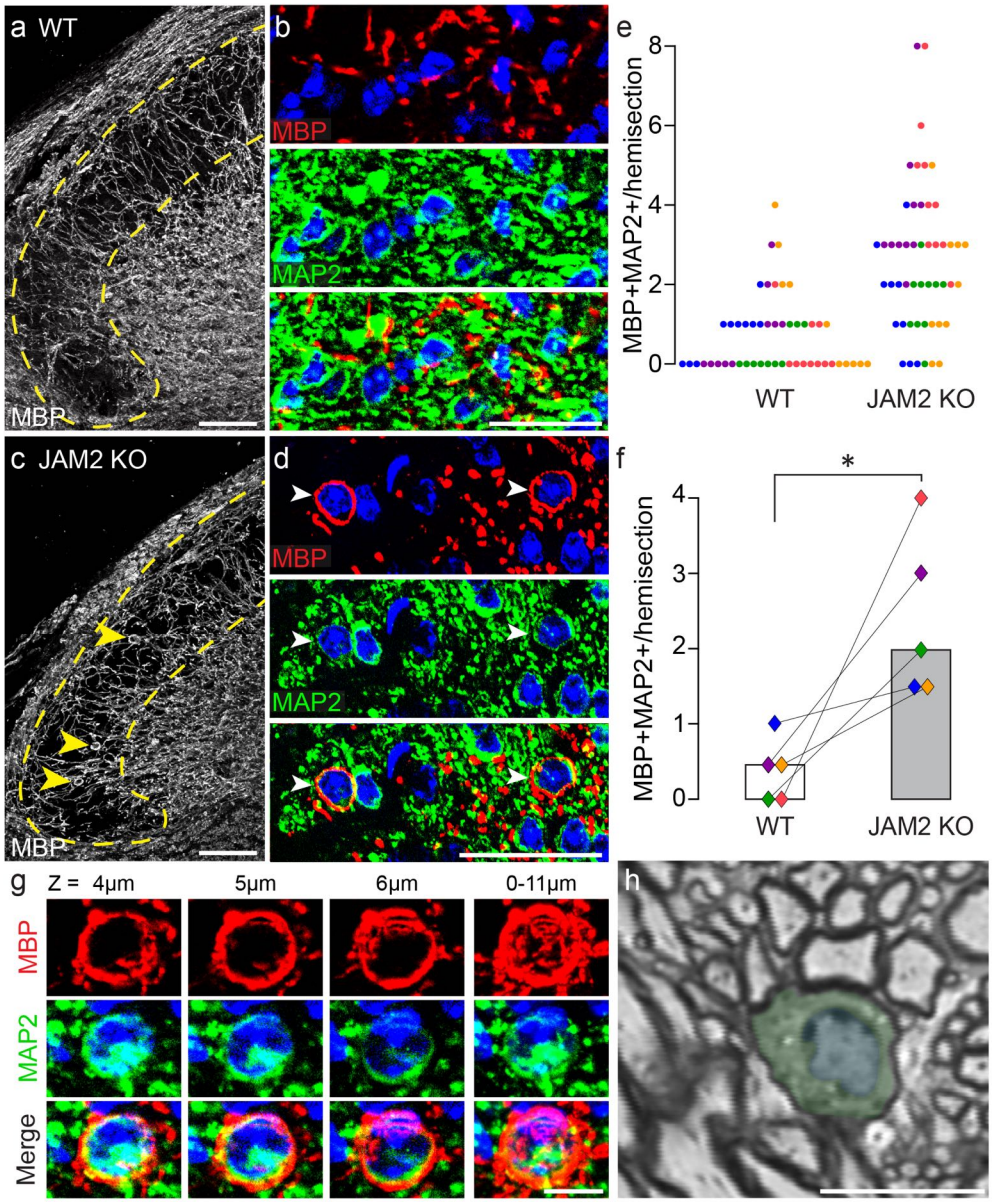

Figure 2-6 | JAM2 is necessary to inhibit somatic wrapping in vivo.

(a) dorsal horn (dotted yellow line) in a coronal section of a wildtype spinal cord immunostained for MBP. (b) higher magnification of dorsal horn myelin (top, red), neurons (middle, green), and merged (bottom). (c-d) same as (a-b) but in JAM2 KO mice. Arrowheads indicate MBP+ wrapped MAP2+ neurons. (e) number of myelin wrapped dorsal horn neurons per hemisection (one dot = one hemisection, colors indicate littermate pairs). (f) bar graph of median number of wrapped neurons per hemisection per mouse. Connected diamonds indicate littermate pairs, and fill color corresponds to dots in (e). n = 5 littermate pairs, median taken from ten hemisections per mouse. *, P = 0.034; Wilcoxon Paired Signed-Ranks test. (g) a myelin wrapped neuron from a JAM2 KO dorsal horn imaged through an 11 micrometer thick z-stack. Individual columns labeled by z-plane depth, and a maximum intensity projection is shown in the far-right column. (h) a toluidine blue stained semi-thin section from a JAM2 KO mouse dorsal horn shows a myelin-wrapped neuron (pseudo-colored green cytoplasm and blue nucleus). Scale bars: (a-d) 50 micrometers, (g-h) 10 micrometers. DAPI, blue.

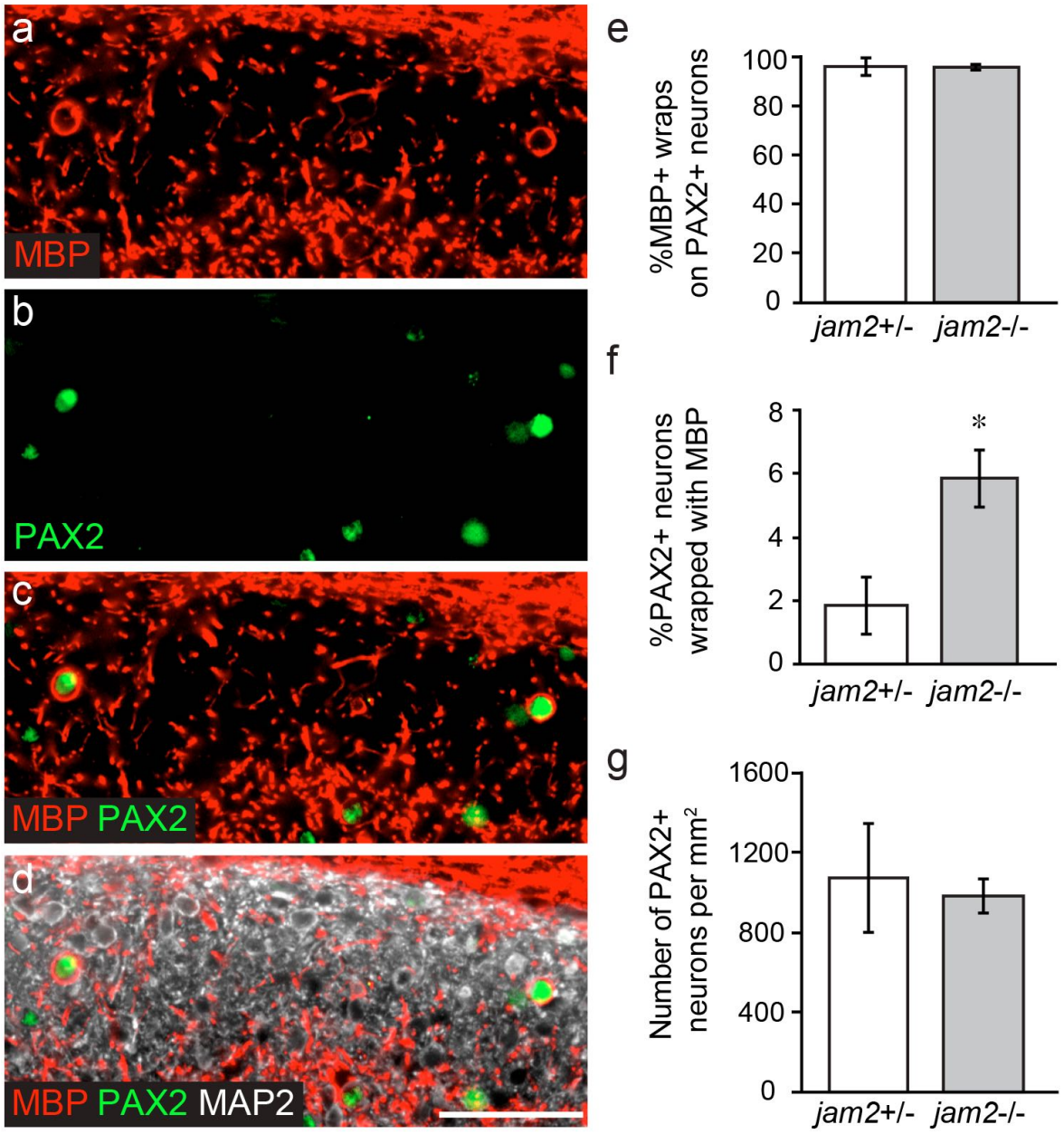

Figure 2-7 | Pax2+ neurons are wrapped in JAM2 knockout mice.

(a) dorsal horn immunostained for MBP, (b) Pax2, (c) label a subset of wrapped (d) MAP2+ neurons. (e) quantification of the percent of MBP+ 'bubbles' on Pax2+ neurons. (f) quantification of the percent of Pax2+ neurons wrapped by MBP+ 'bubbles'. (g) number of Pax2+ neurons per square millimeter in Jam2 +/- and Jam2-/- littermate pairs. n = 4 littermate pairs. Bar graphs represent: (e-f) median calculated as (e) total wrapped Pax2+ out of total wrapped cells per mouse, or (f) percent per field from 10 20x fields per mouse. Error bars represent median absolute deviation; (g) mean density per mouse calculated from 10 20x fields per mouse. Error bars represent s.e.m. *, P = 0.034; Wilcoxon Paired Signed-Ranks test. Scale bar: 50 micrometers.

Discussion

Overall, we show that somatodendritic JAM2 is necessary and sufficient to inhibit oligodendrocyte wrapping. Our results support a model of myelin target selection and wrapping in which pre-myelinating oligodendrocyte processes (Fig 8a) are normally inhibited by somatodendritic cues, including JAM2 (Fig 8b). When such inhibitors are missing, as in JAM2 KO mice, oligodendrocytes form aberrant somatodendritic myelin wraps (Fig 8c). As growing neurons utilize both attractive and repulsive axon guidance cues to precisely target correct brain areas and postsynaptic neurons, our findings indicate that oligodendrocytes utilize somatodendritic inhibition, potentially in addition to axonal attraction, to target myelin segments specifically to axons (Fig 1a, 'Inhibition', 'Mixed').

Inhibitory signals guide oligodendrocyte myelination

The need for inhibitory signaling in tailoring myelination patterns becomes more apparent in neuron-free myelination assays. When oligodendroglia are cultured in the presence of permissive nanofibers, micropillars and spherical beads, they wrap MBP+ myelin membranes around each structure type, including the 50-micrometer diameter circular base of a micropillar (Figs 1c-d, 4c). These results suggest that oligodendroglia have few geometric requirements to form myelin. Indeed, the study of myelination by culturing oligodendrocytes on planar glass coverslips has historically been a successful approach because the cells readily differentiate and form membrane sheets with myelin-like composition in the absence of inductive substrate signaling. Here we use the oligodendrocyte's flexible wrapping requirements to our advantage by adapting the high-throughput micropillar array platform to screen integral membrane protein activity on oligodendrocyte wrapping (Fig 4c-i). Under identical geometric conditions, and in the absence of any other molecular cues, oligodendrocytes and OPCs are dramatically less likely to wrap micropillars coated with JAM2-Fc (Fig 4e-h), and oligodendrocytes form significantly fewer

myelin segments in the presence of soluble JAM2-Fc (Fig 5a-c). Interestingly, the magnitude of JAM2 inhibition is greater on micropillars (66.6%) than in SCN cocultures (24.6%), opening the possibility that axons may express an attractive signal that is able to partially overcome JAM2 inhibition. These results demonstrate the sufficiency of JAM2 to inhibit wrapping, and support the model that oligodendroglial target selection can be regulated by negative and positive microenvironment cues (Fig 1a 'Mixed').

Furthermore, JAM2's inhibition of wrapping is not the result of changes in oligodendroglial cell density or differentiation (Figs 4i; S4c-f). In contrast, previously described inhibitors of axonal myelination negatively affect oligodendroglial cell adhesion *in vitro* and/or oligodendrocyte differentiation *in vitro* and *in vivo* (e.g. LINGO-1, LSAMP) (Lee et al., 2007; Mi et al., 2005; Sharma et al., 2015). It would not necessarily be advantageous for an inhibitor of somatodendritic myelination to prohibit oligodendrocyte differentiation. Oligodendrocytes would still need to differentiate and myelinate gray matter axons that are tightly intermingled with neuron cell bodies and dendrites.

Additional inhibitory myelin guidance molecules

What additional signal(s) prevent aberrant wrapping of other spinal cord neurons and dendrites? JAM2 is widely expressed in the young adult mouse spinal cord (Figs S3, S4a-b). Here we describe the aberrant wrapping of dorsal horn neuron cell bodies. Additional EM analysis of heavily myelinated gray matter areas may reveal that other neuron somatodendritic compartments are wrapped in JAM2 KO mice that are not detectable by immuno- or toluidine blue staining. Nevertheless, it is entirely possible that other neuron types may express other inhibitory molecules in addition to, or instead of JAM2. But even among JAM2-expressing spinal cord motor neurons, it is notable that their dendrites and cell bodies are densely covered with

presynaptic terminals (Molofsky et al., 2014), another normally unmyelinated neuronal structure. Axon terminals, then, may present either a structural barrier preventing oligodendroglial contact with somatodendritic surfaces, or may themselves express a myelination-inhibitory cue that is sufficient to prevent oligodendrocyte wrapping with or without somatodendritic expression of JAM2. Unlike ventral motor neurons, dorsal horn PAX2+ neurons are largely devoid of presynaptic innervation of their somata (Fig S5). Importantly, our data does not distinguish between the possibilities that somatic myelin wrapping removes synapses, or whether only neurons devoid of somatic synaptic terminals are vulnerable to myelin wrapping in the absence of JAM2. In addition to neural sources of myelin inhibition, astrocytes, microglia, oligodendroglia and endothelial cells also remain unmyelinated, and may each express a molecular cue to prevent wrapping.

Oligodendroglial JAM2 receptors

Many receptors in oligodendroglia may be responsible for transducing myelin guidance signals, especially if JAM2 is one of many inhibitory molecules in the CNS. Known JAM2 receptors include other JAM family members JAM1, 2 and 3, as well as integrin alpha-4 beta-1, which may act alone or in combination to bind JAM2 (Arcangeli et al., 2013). In this study, the identity of the JAM2 receptor(s) in oligodendrocytes remains an open question. But if oligodendrocyte differentiation and wrapping are indeed dissociable events as our results suggest (Fig 4e-i), the understanding of downstream mechanisms that separately govern these two processes will be of high interest for future study.

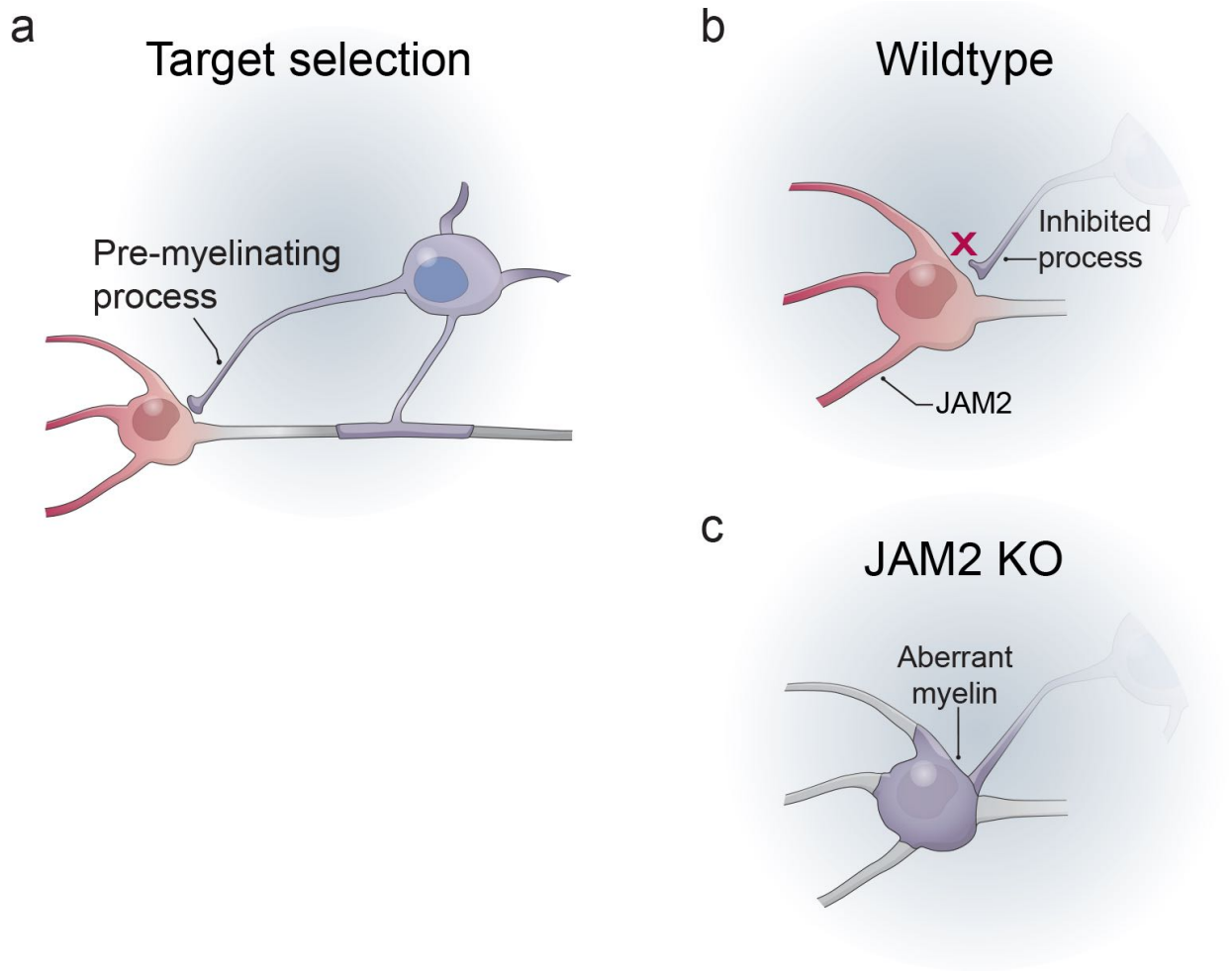

Figure 2-8 | Model of JAM2 function on oligodendrocyte wrapping.

(a) a pre-myelinating process of an oligodendrocyte comes into contact with the somatodendritic compartment of a neuron. (b) in wildtype mice, somatodendritic JAM2 inhibits the oligodendrocyte process from wrapping. (c) when JAM2 is absent or blocked, the oligodendrocyte process is not inhibited, and continues to wrap myelin membranes on the neuron cell body.

Inhibitory myelin guidance molecules and failure of myelin repair

Promoting efficient myelin repair in diseases like multiple sclerosis (MS) has long been a clinical goal. While current therapies aim to control immune infiltration into the CNS, more attention is now being given to directly promoting oligodendrocyte differentiation and remyelination (Mei et al., 2014; Ruckh et al., 2012). However, it has also been observed in human postmortem MS lesions that differentiated oligodendrocytes are present, but fail to remyelinate axons (Chang et al., 2002). Could inhibitory myelin guidance molecules be aberrantly upregulated or mislocalized in MS lesions and prevent efficient repair? If so, it is essential to identify such signals, as they may be feasible targets to block and promote myelin repair. As additional myelin guidance molecules are identified, it will be important to understand their roles in both myelin formation and regeneration.

Chapter Three: Revitalizing Remyelination—the Answer Is Circulating

Walled off by bone and the blood-brain barrier, the central nervous system (CNS) is protected from many physical and chemical dangers that threaten more exposed tissues. But while many tissues heal and regain function after injury or disease, the nervous system is notoriously poor at repair, even more so as we age. Because the CNS operates in near isolation from other systems, its failure to repair and regenerate has long been attributed to cell-intrinsic shortcomings that become more limited over time. But Ruckh *et al.* (2012) suggest that cells of the CNS may not be so intrinsically limited in repair and that enhancing exposure of the damaged brain or spinal cord to beneficial factors in the blood could aid recovery in injury and disease.

Why does the capacity for CNS repair degenerate with age? In the autoimmune disease multiple sclerosis, for instance, it is thought that remyelination of neuronal axons is painfully slow and incomplete in adults because oligodendroglia (myelin-producing cells of the CNS) are increasingly less sensitive to promyelinating cues (Shen *et al*., 2008). But Ruckh *et al.* (2012) show that the remyelination potential of oligodendroglia in demyelinated spinal lesions of old mice is boosted by recruitment of peripheral circulating innate immune cells (macrophages) from young mice. The authors induced a demyelinated lesion in an old mouse to assess remyelination over time. They uncoupled oligodendroglial cell-intrinsic factors from systemic factors in blood that may affect remyelination by using heterochronic parabiosis, a surgical technique that joins the circulatory system of an old wild-type mouse with that of a young mouse (genetically engineered to ubiquitously express green fluorescent protein). If adult-derived oligodendroglia intrinsically lose remyelination capacity as the animal ages, exposing the lesion to circulating blood from a young mouse would not affect the extent of remyelination.

Surprisingly, the old-young mouse pairs exhibited enhanced remyelination that depended on the recruitment of circulating macrophages from the young mouse. Exposure to the young mouse circulation is also required, as genetically preventing “young” macrophage recruitment only partially prevented the effect. These results suggest that resident “old” oligodendroglia retain considerable potential to proliferate, differentiate, and remyelinate even as they age, but age-related changes in the systemic milieu and reductions in resident and/or recruited macrophage phagocytic capacity restrict this reparative potential (Figure 1).

Little is known about aging effects on the immune system, but it has been suggested that macrophages become less efficient with age and their decreased activity may contribute to age-related chronic inflammation (Shen *et al*., 2008; Durafourt *et al*., 2012). This, combined with lower efficacy of pathogen clearance, could result in prolonged exposure of CNS cells to harmful amounts of detrimental cytokines. Recently, similar heterochronic parabiosis experiments identified increased concentrations of the cytokine CCL11 in healthy aged mice as sufficient to inhibit adult neurogenesis in young mice and induce cognitive deficits (Villeda *et al.,* 2011).

Additionally, the accumulation of cellular debris and/or plaques (insoluble fibrous protein aggregates) in the CNS is thought to inhibit neuronal repair and regeneration, as well as promote degeneration. For example, the accumulation of brain β-amyloid plaques in Alzheimer's disease leads to neuronal death and cognitive deficits. Consistent with the findings by Ruckh *et al.* (2012), stimulating phagocytic clearance of β-amyloid protects against neuronal death and facilitates cognitive recovery (Cramer *et al.*, 2012). Ruckh *et al.* (2012) suggest a link between age-related accumulation of damaged-myelin debris and remyelination failure. Such debris may be wrongly interpreted as healthy myelin, which might attenuate oligodendroglial proliferation,

migration, and/or differentiation, resulting in a shortage of remyelinating oligodendrocytes (Franklin *et al.*, 2002; Chong *et al.*, 2012; Kotter *et al.*, 2006).

Maximizing macrophage recruitment to demyelinated lesions may be one avenue to support remyelination. Both CNS microglia (resident macrophages of the brain) and recruited macrophages are polarized to the anti-inflammatory, highly phagocytic "M2" activation state in demyelinated lesions, releasing cytokines that may also directly support remyelination (Durafourt *et al.*, 2012; Schechter *et al.*, 2009). "Young" macrophages recruited to "old" lesions may rescue age-related decreases in the phagocytic capacity of "old" macrophages or in their secretion of cytokines that promote repair.

The study by Ruckh *et al.* (2012) suggests that the age-related deficits in remyelination are not solely attributable to the cell-intrinsic capacity of "old" oligodendroglia, but are influenced by extrinsic factors outside the brain and spinal cord. Whether remyelination-promoting serum factors are contributed by the young mouse or remyelination-inhibitory serum factors from the old mouse are sufficiently diluted as a result of parabiosis to allow for enhanced remyelination remains to be determined. The nature of the effect of the youthful macrophages (if any) on the activation of endogenous older microglia, and the cytokine(s) involved, also should be clarified. Such further characterization would provide valuable insight into the aging immune system.

The findings of Ruckh *et al.* (2012) suggest that maximizing intrinsic oligodendroglial myelinogenic potential by altering the local lesion environment could be a promising therapeutic target to promote repair in diseases such as multiple sclerosis. Whereas research concerning myelin repair has traditionally focused on dampening the immune system and promoting differentiation of oligodendroglia, it may be that the keys to efficient remyelination reside in the circulation.

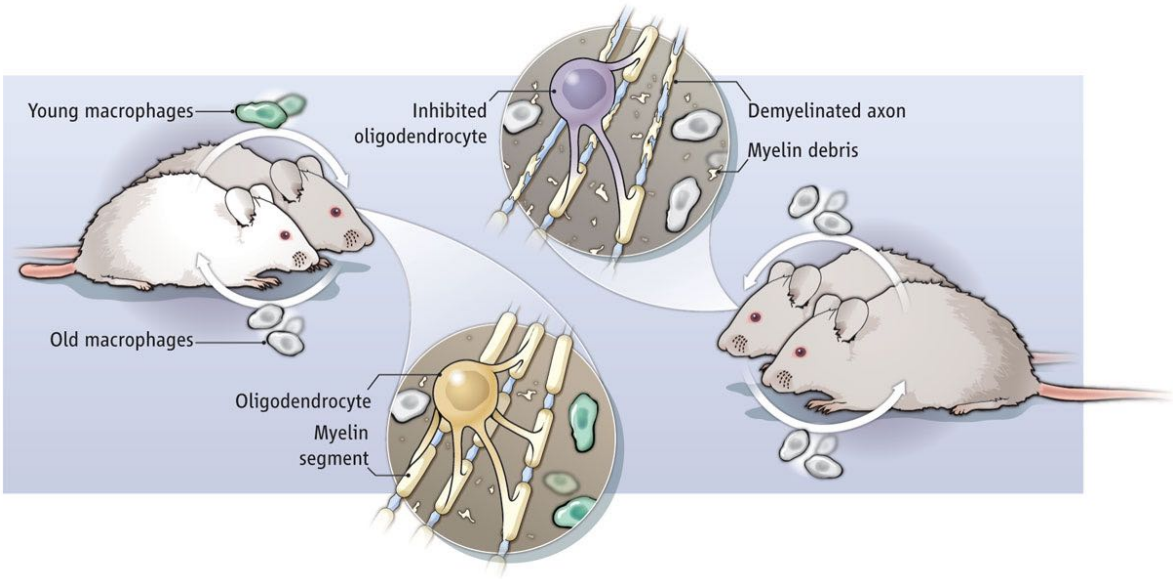

Figure 3-1 | Reversing Aging Effects

The circulatory system of an “old” mouse (gray) with a demyelinated lesion was surgically joined with that of a healthy “young” mouse (white) (Ruckh *et al.*, 2012). The old mouse exhibited enhanced remyelination relative to the control, an old-old mouse pair. Remyelination depended on the recruitment of circulatory factors from the young mouse, including macrophages. Resident “old” oligodendroglia retain remyelination potential even as they age, but macrophage-mediated clearance of inhibitory myelin debris from the lesion may become impaired.

Conclusion

One of the great barriers to understanding myelination has been the traditional methods used to study it. Antibody labeling, fluorescence and electron microscopy are all static methods of visualizing myelin formation. Oligodendrocyte precursor cells (OPCs) are multiprocessed cells that are highly dynamic and migratory before they differentiate into myelinating oligodendrocytes (Hughes et al., 2013). The adult OPCs imaged through a cranial window in Hughes, et al (2013) were highly processed, but only a subset of the process tips developed into myelin segments when the OPCs differentiated. It is well appreciated that myelin only forms around the axons of neurons (Lubetzki et al., 1993), but what OPCs are contacting, which processes are preserved to become myelin internodes, and which are destined to be pruned away are still open questions.

We began this thesis with the question; *why are dendrites not myelinated?* We found that OPCs and oligodendroglia wrapped plastic nanofibers above a threshold diameter (Lee et al., 2012). Dendrites of similar diameter, however, remain unmyelinated in vitro (see Figure 2-2) and in vivo. Are unmyelinated dendrites contacted and rejected by OPC or oligodendrocyte cell processes, or do they lack an attractive cue required to induce myelination of neurons? We found that by cross-linking surface proteins of cultured neurons, oligodendrocytes wrapped myelin membranes around dendrites and neuron cell bodies in addition to axons (see Chapter Two). This result led us to hypothesize that neuron cell bodies and dendrites express a myelination-inhibitory cue. Ultimately, we found that JAM2 is necessary to inhibit myelination of neuron cell bodies and dendrites, and is sufficient to reduce the number of myelin segments formed per oligodendrocyte in vitro (see Chapter Two).

We categorized JAM2 as a myelin guidance molecule, as it 'guides' the correct formation of myelin in the nervous system. More broadly, myelin guidance molecules as a class are likely necessary to communicate neuron cell polarity to oligodendrocytes as they myelinate. Many other structures in the central nervous system fall into 'myelinated' or 'unmyelinated' categories, despite their geometric permissivity: OPCs, oligodendrocytes, astrocytes, microglia, vasculature, ependymal cells, neural stem cells, neuron synapses, axon initial segments, nodes of Ranvier, and even some axons. It will be interesting to see whether inhibitory myelin guidance molecules are required to establish and maintain the unmyelinated status of these cells and subcellular structures.

Finally, what role(s) attractive and/or inhibitory myelin guidance molecules play in remyelination remains to be seen. In cases of multiple sclerosis, demyelinated lesions can become chronically demyelinated. There is a possibility that inhibitory cues are mislocalized or misexpressed in such lesions that prevent efficient remyelination. Inhibitory myelin debris (see Chapter Three; Ruckh et al., 2012) is an example of such a 'mislocalized' signal that prevents repair. When immune cells from younger mice phagocytosed this left-over debris, Ruckh et al. (2012) found that remyelination was significantly improved. If inhibitory myelin guidance cues present on myelin debris or on other structures within a demyelinated lesion can be identified, the possibility exists that such cues could be targeted with novel therapeutics, allowing OPCs to more efficiently infiltrate the lesion, differentiate and reform myelin.

Experimental Procedures

Animals

All animals used in this study were housed and handled with the approval of the University of California San Francisco Institutional Animal Care and Use Committee (IACUC). Timed-pregnant Sprague-Dawley rats were procured from Charles River Laboratory (Strain No: 400, RRID:RGD_734476). Dorsal root ganglion neuron and spinal cord neuron dissections were done on embryonic day 15. Junction Adhesion Molecule 2 (JAM2) knockout mice are as previously described (Arcangeli et al., 2011, MGI:5779544). The *jam2:beta-galactosidase* knock-in mice were purchased from Jackson Laboratory (B6N(Cg)-Jam2$^{tm1.1(KOMP)Mbp}$/J, Stock No: 024055, MGI:5522546). Jam2 knockout mice were used to generate data in Figures 5-6, S3-S4, and B6N(Cg)-Jam2$^{tm1.1(KOMP)Mbp}$/J mice were used to generate data in Figures 7, S2 and S5.

Immunohistochemistry

Cell cultures were immunostained with standard techniques, discussed elsewhere in detail (Lee et al., 2013). Briefly, cultures were fixed with 4% paraformaldehyde (Electron Microscopy Tools) in DPBS (Life Technologies), washed with PBS, air dried, then blocked and permeabilized in 20% normal goat serum (NGS) (Sigma-Aldrich) plus 0.1% Triton X-100 (Sigma-Aldrich) in DPBS. The cultures were incubated in 20% NGS in dPBS plus primary antibodies. Cultures were washed in PBS, and incubated in 20% NGS in dPBS plus secondary antibodies. The cultures were washed in PBS then distilled water, air dried and then mounted on microscope slides with Fluorescence Mounting Medium (Dako).

Spinal cord tissue was collected from P30-33 mice using standard techniques. Briefly, after transcardial perfusion with PBS and then 4% paraformaldehyde (Electron Microscopy Tools),

the spinal cord was dissected out and post-fixed in 4% paraformaldehyde overnight at 4° Celsius and cryoprotected by incubation in 30% sucrose in PBS until tissue sank. Coronal sections were cut in 30-micrometer thick slices from the cervical spinal cord (C5-C8) using a freezing microtome (Microm HM 450 and KS 34, Thermo Scientific). Sections were immunostained with the same methods as cell cultures above.

Images were collected using a Zeiss Axio Imager Z1 Apotome or M2 Apotome.2 fluorescence microscope with either Axiovision or Zen software (Zeiss). Images are shown as a maximum intensity projection of optical section z-stacks. Micropillar cultures (Mei et al., 2014) and semi-thin sections were imaged using a Zeiss LSM-700 confocal microscope and Zen software.

Antibodies

Antibodies used for immunostaining are: microtubule associated protein 2 (chicken anti-MAP2, 1:1,000, Millipore Cat# AB5543, RRID:AB_571049); neurofilament (mouse anti-NF, 1:200, Covance Cat# SMI-312R, RRID:AB_10119994); junction adhesion molecule 2 (rabbit anti-JAM2, 1:100-200, ThermoFisher Scientific Cat# PA5-21576, RRID:AB_11156435); myelin basic protein (rat anti-MBP, 1:100, Millipore Cat# MAB386, RRID:AB_94975); p75-neurotrophin receptor (mouse anti-p75NTR, 1:25 hybridoma cell line gift of E.M. Shooter lab, clone MC192, commercially available as RRID:AB_528539); contactin associated protein (mouse anti-CASPR, 1:500, E. Peles laboratory, RRID:AB_2314218), neuronal nuclei (rabbit anti-NeuN, 1:2000 Abcam Cat# ab177487, RRID:AB_2532109), adenomatous polyposis coli (mouse anti-APC/CC1, 1:200 Millipore Cat# OP80, RRID:AB_2057371), beta-galactosidase (chicken anti-βGal, 1:1000 Aves Labs Cat# BGL-1040, RRID:AB_2313507), vesicular glutamate transporter 2 (guinea pig anti-VGLUT2, 1:4,000 Millipore Cat# AB2251, RRID:AB_1587626), vesicular glutamate transporter 1 (guinea pig anti-VGLUT1, 1:4,000 Synaptic Systems Cat#135 304,

RRID: AB_887878), vesicular GABA transporter (guinea pig anti-VGAT, 1:500 Synaptic Systems Cat# 131 004, RRID:AB_887873), paired box gene 2 (rabbit anti-PAX2, 1:1,000-4,000 Abcam Cat# ab79389, RRID:AB_1603338), and platelet derived growth factor receptor-alpha (rabbit anti-PDGFRα, 1:8,000, generous gift of W.B. Stallcup, Sanford-Burnham Medical Research Institute, Cancer Center, La Jolla, CA USA, RRID:AB_2315173). Secondary antibodies were Alexa Fluor raised in goat against rat, mouse, rabbit, human or chicken in the following wavelengths: 488, 594, 647 (1:1,000 Life Technologies) and nuclei were stained with DAPI. The antibodies used in function-blocking experiments (Figure S1): rat anti-JAM2 (5µg/mL, R&D Systems MAB9881, RRID:AB_2128924) or rat IgG (5µg/mL, R&D Systems 6-001-F, RRID:AB_2616570).

Primary neuron and glia isolation and culture

Spinal cord neuron (SCN) isolation and culture has been described previously (Camu and Henderson, 1992; Molofsky et al., 2014). Briefly, embryonic day 15 rat or mouse embryo spinal cords were dissected and meninges removed as much as possible. Spinal cords were chopped with a sterile scalpel blade and the tissue was incubated in 0.05% trypsin-EDTA (Life Technologies) for 15 minutes at 37° Celsius. The tissue was dissociated into a single-cell suspension and incubated in a series of immunopanning dishes; two negative selection dishes coated with monoclonal hybridoma antibodes rat neural antigen-2 (Ran-2, ATCC) and Galactocerebrocide (Gal-C (Ranscht et al., 1982)); and one positive selection plate against p75 neurotrophin receptor (p75NTR, rat cells: MC192 hybridoma; mouse cells: rabbit anti-p75 function blocking antibody ‘REX’, a generous gift of L.F. Reichardt (Weskamp and Reichardt, 1991)). Adherent cells were released from the final immunopanning plate with a brief application of 0.05% trypsin-EDTA and 200,000-300,000 cells were seeded on 25mm round coverslips prepared with 200µL of 1:25 Matrigel (Corning, 356230) in DMEM (Life Technologies). SCN

were left to adhere overnight, and flooded with growth medium plus 5-fluoro-2'-deoxyuridine (FDU) to kill mitotic cells, and 80% of growth medium was changed every three days for 3-4 weeks: DMEM (Life Technologies), B27 (Life Technologies), N2 (Life Technologies), penicillin-streptomycin (Life Technologies), N-acetylcisteine (NAC, Sigma-Aldrich), forskolin (EMD), insulin (Sigma-Aldrich), brain-derived neurotrophic factor (BDNF, Peprotech), ciliary neurotrophic factor (CNTF, Peprotech), glial-derived neurotrophic factor (GDNF, Peprotech).

Dorsal root ganglion (DRG) neuron cultures were established as previously described (Mei et al., 2014). Oligodendrocyte precursor cells (OPCs) were isolated (Lee et al., 2013) and cultured on micropillars as previously described (Mei et al., 2014).

OPCs were cocultured with 3-4 week old SCN as follows: OPCs were isolated with hybridoma anti-A2B5 or anti-O4-coated panning dishes, and 400,000 OPCs were seeded on each SCN culture in chemically-defined medium (Lee et al., 2013), which was changed every three days. For Jam2-Fc or Fc cocultures (Figure 5), 10 micrograms/mL protein was added to culture medium.

Oligodendrocyte nanofiber and microbead culture

Aligned polycaprolactone nanofibers were purchased in an 8-chamber slide format (Nanofiber Solutions cat 0802). 20 micrometer-diameter NH_2 polystyrene beads (Kisker Biotech Gmbh & Co cat PPS-20.0NH2) were sparsely seeded into the nanofiber chambers, coated with poly-L-lysine and dried to promote adhesion of beads to the nanofibers. OPC culture on beads and nanofibers was performed essentially as described (Chong et al., 2012; Lee et al., 2013). OPCs were seeded into the chambers and cultured for 3-4 days, then fixed and immunostained as above.

Oligodendrocyte coculture on live and cross-linked SCNs

SCN cultures were established as above. Prior to OPC seeding, SCN cultures were chemically cross-linked as described (Rosenberg et al., 2008) with 4% paraformaldehyde for 10 minutes at room temperature. Fixed neuron cultures were extensively washed in L15 medium + 10% FBS (Gibco), and finally washed with coculture medium. One million OPCs were seeded onto either live or cross-linked neurons and cocultured for 5 days (Figure 2) or 7-12 days (Figure 1) in a chemically defined medium, then immunostained as above.

Micropillar protein coating

Micropillar arrays were sterilized with 100% ethanol and dried. Micropillars were coated with poly-L-lysine for one hour at room temperature, washed three times with water and dried. Each micropillar array of 1000 pillars was then coated with 2µg of either Fc protein (R&D Systems 110-HG, RRID:AB_276244) or JAM2-Fc protein (R&D Systems 988-VJ-050) in 27µL Tris HCl pH 9.5 overnight at room temperature. The micropillars were washed three times with water and twice with oligodendrocyte culture medium and kept wet with medium until 40,000 OPCs were seeded.

JAM2-Fc and Fc protein binding assay

OPCs were seeded onto poly-L-lysine coated coverslips in PDGF-containing culture medium overnight. On div 3, coverslips were washed with DMEM and incubated in 2µg/mL JAM2-Fc or Fc in DMEM for 30 minutes at room temperature. The coverslips were washed three times with DPBS, fixed with paraformaldehyde and immunostained as above.

Western Blot Analysis

Western blotting was performed essentially as previously described (Rosenberg et al., 2008). 25mm coverslips containing either SCN alone or myelinating SCN cocultures were collected in 100µL/coverslip of ice cold RIPA buffer, kept on ice and frozen immediately at -80°C. Samples were thawed on ice and homogenized. Protein concentration was determined by BCA Protein Assay (Thermo Scientific 23225). Proteins were transferred to pure nitrocellulose membranes and probed with primary antibodies (see Antibodies) and Alexa Fluor 680 secondary antibodies raised in goat (Life Technologies). Imaging was conducted with an Odyssey infrared system (LI-COR).

RNA isolation, RNA sequencing and bioinformatics

Spinal cords and dorsal root ganglia were dissected from a single litter of embryonic-day 15 rat embryos, SCN and DRG neurons were isolated and cultured for three weeks as described above. RNA was isolated using Trizol Reagent and manufacturer's protocol (Life Technologies). Sequencing was performed with Illumina Genome Analyzer Sequencing System. Over 142M single end reads of length 100 bases were sequenced per sample. Sequences were produced with CASAVA (version 1.8.1.) and aligned to Rattus norvegicus rn4 genome build using TopHat (version 1.3.0) (Trapnell et al., 2009). TopHat was run separately for each RNA-Seq library with the options "--segment-mismatches 1 --min-intron-length 30 --max-multihits 10 --solexa-quals -o". Transcriptome was assembled using Cufflinks (Roberts et al., 2011; Trapnell et al., 2010) (version 1.1.0) and RefSeq reference annotation file (using the options –g).The reference was downloaded from the UCSC tables. The two assembled transcriptomes were merged with the tool Cuffmerge (version 1.1.0.). Cuffdiff was used to detect differentially expressed genes and transcripts between the two samples. Identification of the rat transcripts coding for membrane and transmembrane proteins was done with Ingenuity® Pathway Analysis (IPA®). The criteria

for selection of differentially expressed transcripts was a higher expression in SCNs as compared to DRGs, and q values <=0.05.

Quantitative PCR

Total RNA was extracted from three-week-old spinal cord neuron or dorsal root ganglion neuron cultures using Trizol Reagent (Life Technologies), and precipitated using either chloroform and isopropanol or PureLink RNA Mini Kit (Life Technologies, cat. 12183020). RNA was reverse transcribed using the RETROscript kit oligo-dT primers (Thermo Fisher, cat. AM1710). cDNA was amplified in triplicate using Power SYBR Green PCR master mix (Thermo Fisher, cat. 4367659) and primers for either *jam2* (Forward 5' TACTGTGAAGCCCGCAACTC 3', Reverse 5' GCAGAAATGACGAAGGCCAC 3', product length 122 base pairs), or *gapdh* (Forward 5' GTGCCAGCCTCGTCTCATAG 3', Reverse 5' AGAGAAGGCAGCCCTGGTAA 3', product length 91 base pairs). qPCR was run on a 7500 Real Time PCR system and analyzed with 7500 software version 2.0.6 (Applied Biosystems).

Electron microscopy

Transmission electron microscopy of cell cultures is as described previously (Lee et al., 2013; Rosenberg et al., 2008). Briefly, cultures were fixed with 4% PFA (Electron Microscopy Tools), incubated in 1% osmium tetroxide (Electron Microscopy Tools), then counterstained with 1% uranyl acetate. Samples were dehydrated in a series of ethanol dilutions and embedded in 1:1 EMBed-812 resin (Electron Microscopy Sciences) to propylene oxide (PPO, Electron Microscopy Sciences), then incubated in a 2:1 resin to PPO mixture. Cultures were detached from the coverslip with a razor blade and rolled tightly before embedding into the final 100% resin block. Ultrathin sections were cut at the W.M. Keck Foundation Advanced Microscopy Laboratory and imaged with a JEM1400 Electron Microscope (JEOL) in the Zilkha Neurogenetic

Institute. Scanning electron microscopy of micropillars is as described previously (Mei et al., 2014).

Image analysis and statistics

The UCSF department of Biostatistics was consulted to identify suitable statistical tests. Statistical significance was determined at P-values < 0.05. Statistical tests were applied as described in figure legends. Data normality was determined using the Kolmogorov–Smirnov test. N values are indicated in the figure legends.

Supplemental Figures

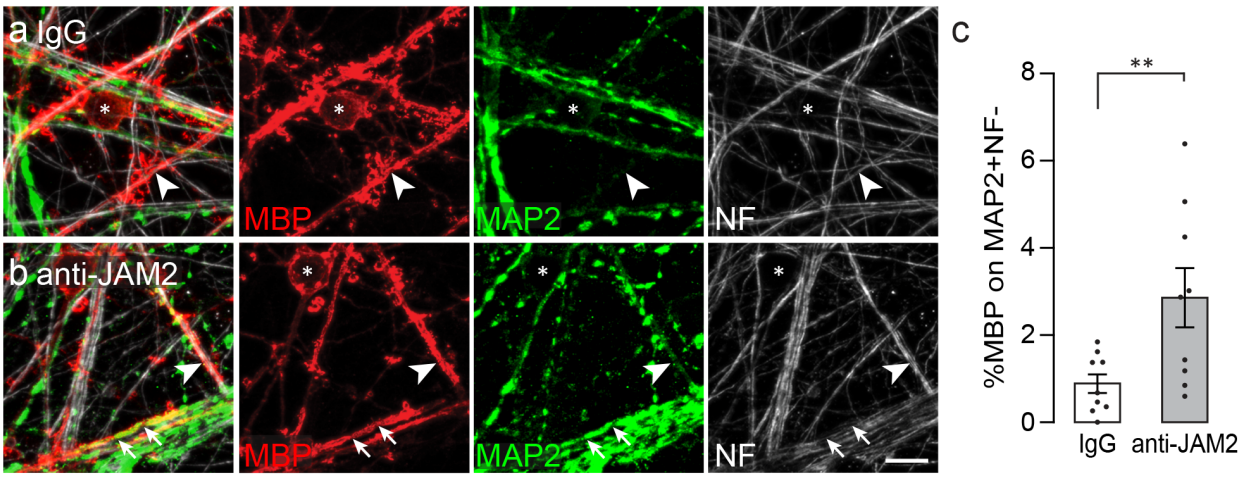

Figure 0-1 | JAM2 function is necessary to prevent dendritic wrapping in vitro.

(a) 7div myelinating SCN cultures incubated for the final two days with either IgG or (b) anti-JAM2 function blocking antibody. Oligodendrocytes (asterisks) wrap myelin membranes on axons (arrowheads) and on dendrites (arrows). (c) the percentage of MBP+ myelin segments on MAP2+/NF- dendrites. Bar graphs represent means with s.e.m. error bars. Significance was calculated using one-tailed Students t-test. **, P = 0.0072. Scale bar: 10 micrometers.

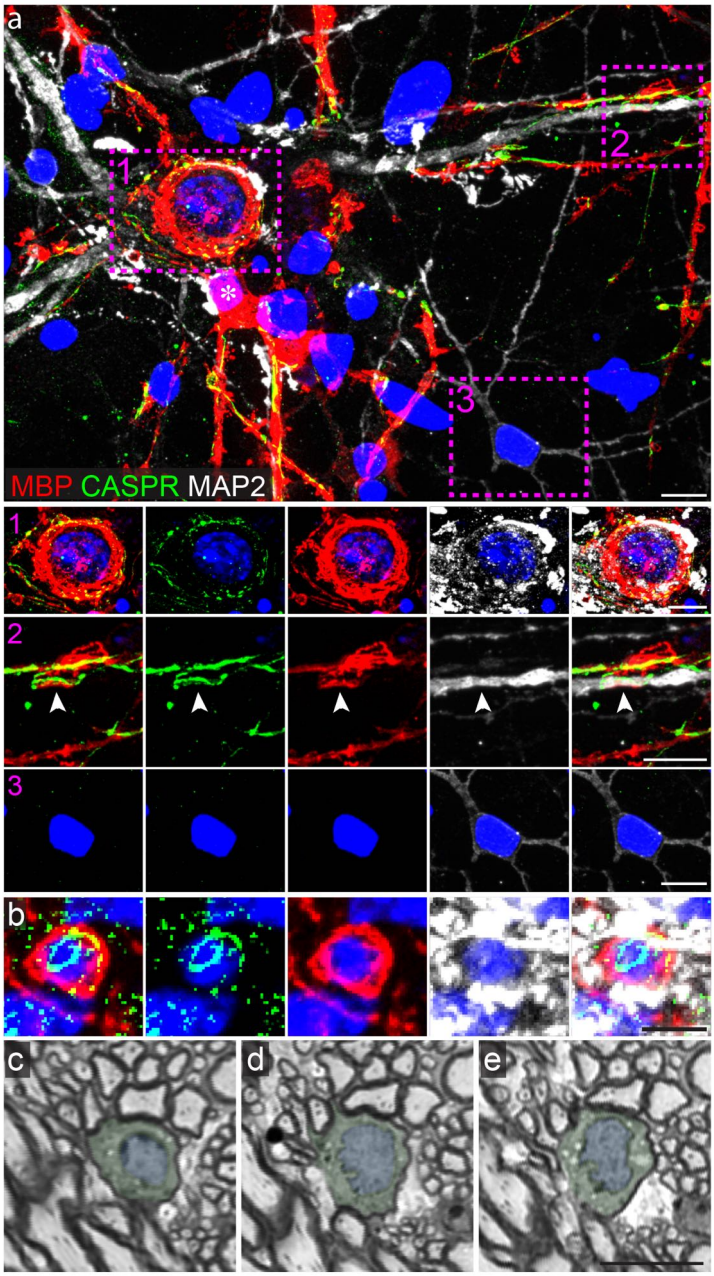

Figure S-2 | Oligodendrocyte ensheathment of JAM2 KO neurons in vitro and in vivo clusters somatodendritic CASPR protein.

(a) a myelinating SCN coculture immunostained for MBP (red), CASPR (green) and MAP2 (white). Insets demonstrate examples of (a1) clustered CASPR on a wrapped neuron cell body, (a2) clustered CASPR on a wrapped dendrite, and (a3) no clustered CASPR signal on an unwrapped MAP2+ neuron. (b) a MAP2+ JAM2 KO dorsal horn neuron is wrapped *in vivo* by an MBP+ oligodendrocyte. At the edges of the MBP+ membrane is a spiraling line of clustered CASPR protein on the neuron surface. (c-e) a myelin-wrapped dorsal horn JAM2 KO neuron in three adjacent semi-thin sections stained with toluidine blue. The neuron cytoplasm is pseudo-colored green, and its nucleus is pseudo-colored blue. DAPI, blue. Scale bars: (a-c) 10 micrometers.

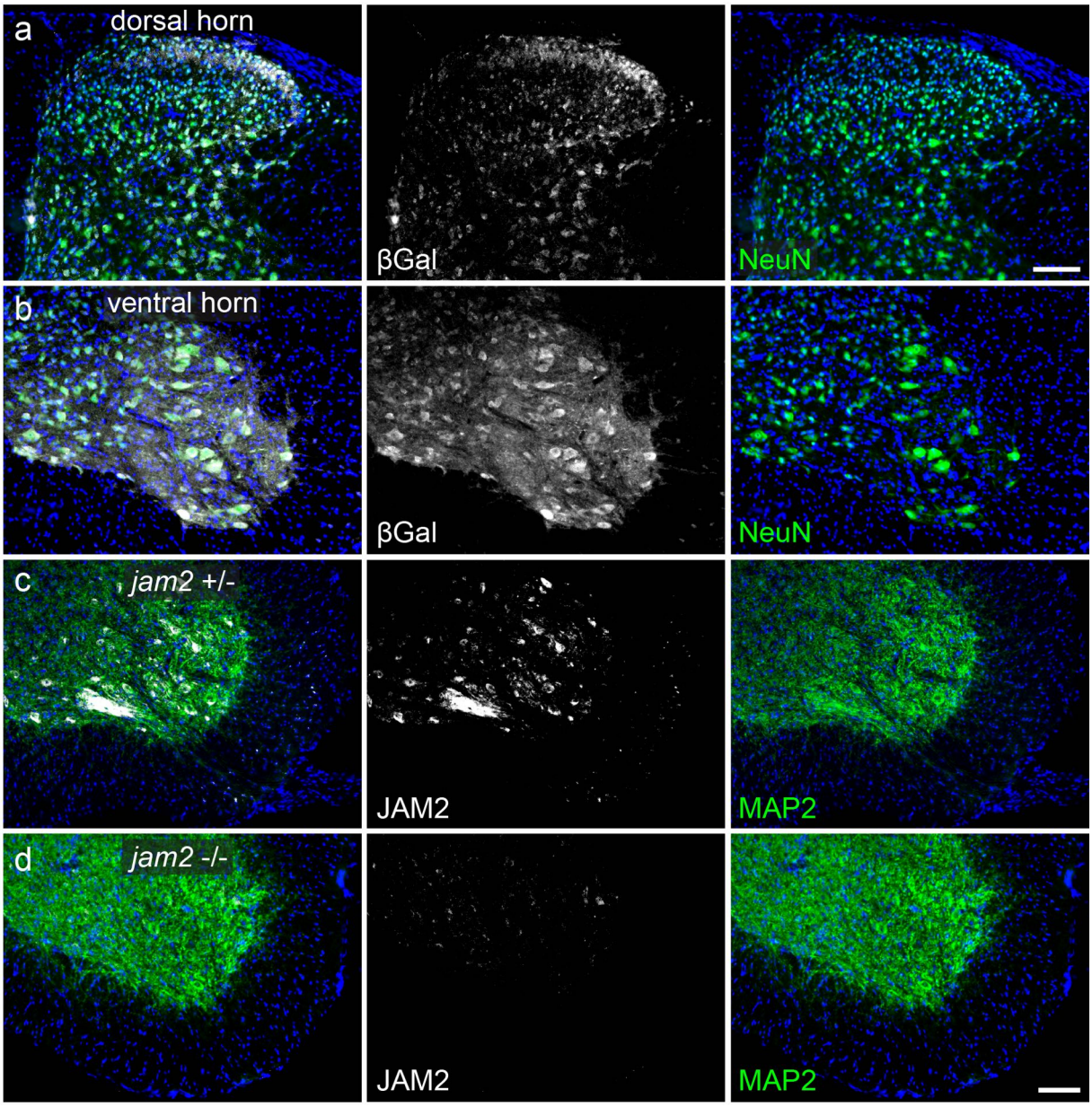

Figure S-3 | JAM2 is widely expressed in spinal cord gray matter.

Low-field images of the (a) dorsal and (b) ventral horns in a heterozygous *jam2:beta-galactosidase* knock-in reporter mouse shows widespread colocalization of NeuN+ beta-galactosidase+ cells. The ventral horns of (c) *jam2* heterozygous and (d) knockout mice show the presence of JAM2 protein on large neurons in MAP2+ gray matter. DAPI, blue. Scale bars: 50 micrometers.

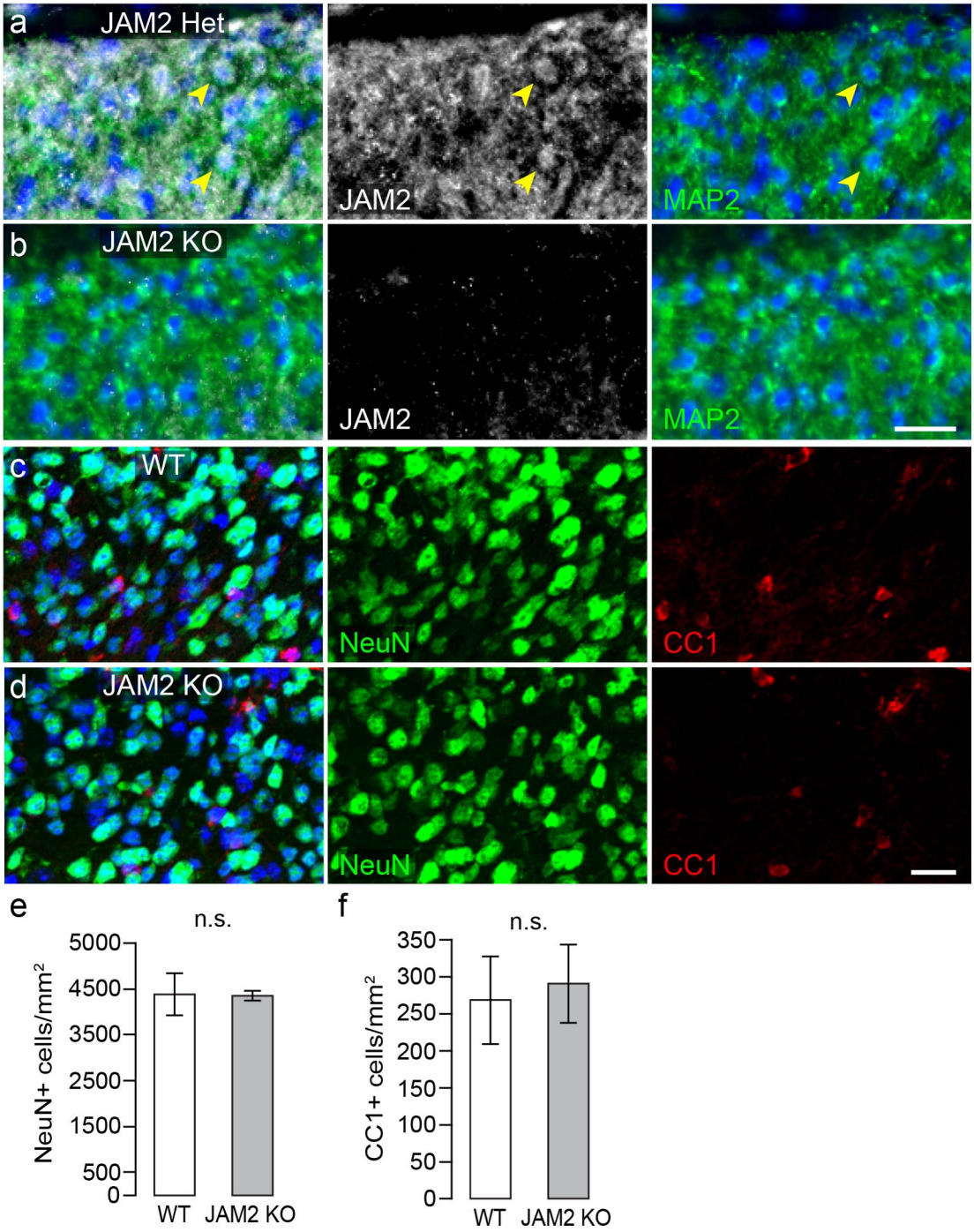

Figure S-4 | The spinal cord dorsal horn develops normally in JAM2 KO mice.

Cross-sections of (a) JAM2 heterozygous (JAM2 Het) and (b) JAM2 KO show specific antibody labeling of JAM2 (white) on MAP2+ neuron cell bodies (arrowheads) in dorsal horn gray matter. In the dorsal horns of (c) WT and (d) JAM2 KO mice the densities of NeuN+ neurons and CC1+ oligodendrocytes is not significantly different. Quantification of (e) NeuN+ and (f) CC1+ cells in WT and JAM2 KO mouse dorsal horns. Bar graphs represent means with s.e.m. error bars. n = 3 littermate pairs. Significance was calculated using the paired two-tailed Students t-test. DAPI, blue. Scale bars: 20 micrometers.

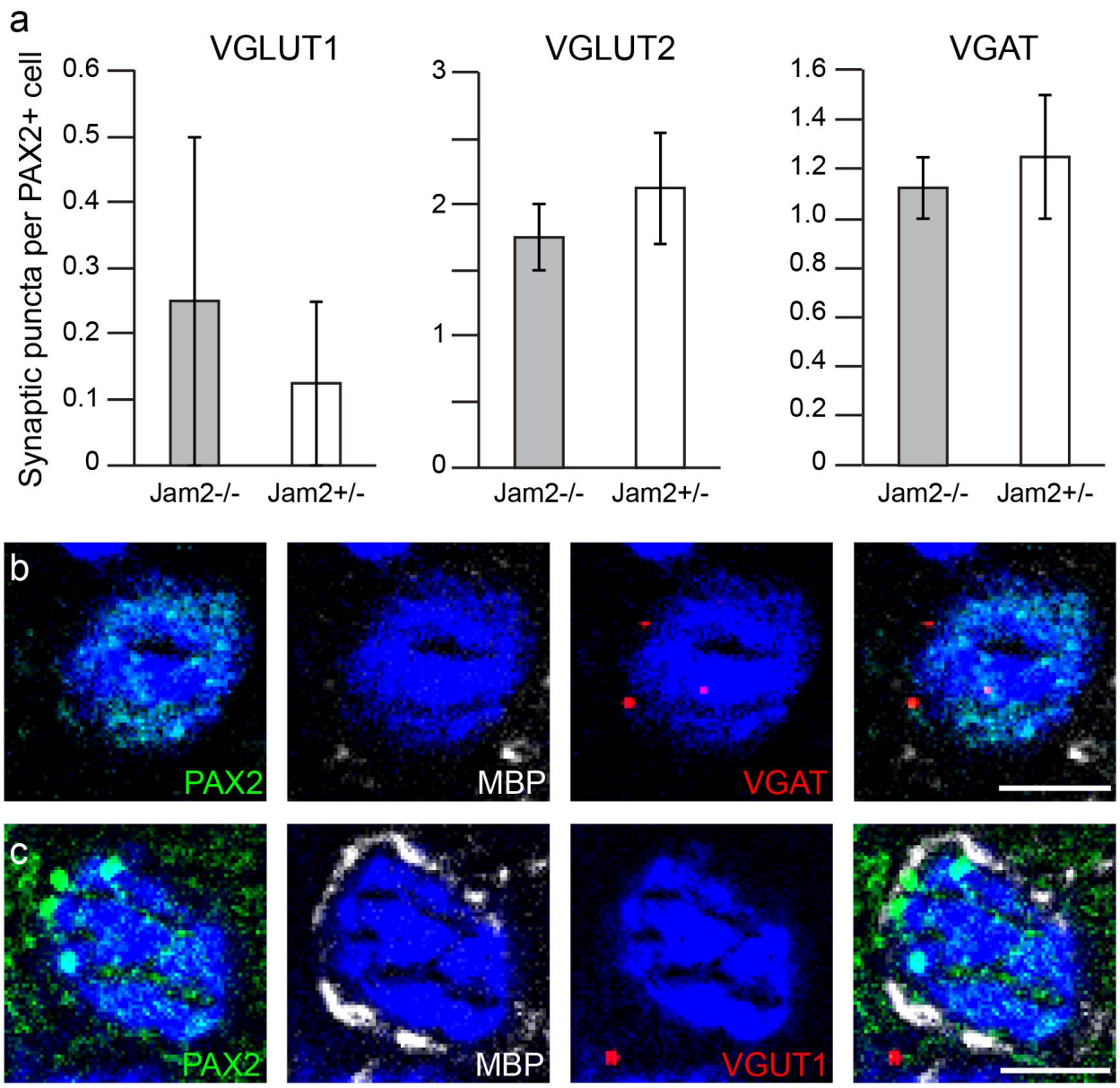

Figure S-5 | Pax2+ dorsal horn neurons have no or few somatic synapses in vivo.

Quantification of the number of (a) VGLUT1, VGLUT2 or VGAT synapses onto PAX2+ neuronal somata in Jam2 -/- or Jam2 +/- mice. (b) VGAT puncta on a Pax2+ neuron soma. (c) a Pax2+ neuron wrapped by MBP+ membrane has no VGLUT1+ synaptic puncta on its soma. Bar graphs represent mean with s.e.m. error bars. n = 4 littermate pairs. Significance was calculated using the two-tailed Mann-Whitney U test. Scale bars: (b-c) 10 micrometers.

References

Aggarwal, S., Snaidero, N., Pähler, G., Frey, S., Sánchez, P., Zweckstetter, M., Janshoff, A., Schneider, A., Weil, M.T., Schaap, I.A., et al. (2013). Myelin membrane assembly is driven by a phase transition of myelin basic proteins into a cohesive protein meshwork. PLoS Biol 11, e1001577.

Aggarwal, S., Yurlova, L., Snaidero, N., Reetz, C., Frey, S., Zimmermann, J., Pähler, G., Janshoff, A., Friedrichs, J., Müller, D.J., et al. (2011). A size barrier limits protein diffusion at the cell surface to generate lipid-rich myelin-membrane sheets. Dev Cell 21, 445-456.

Arcangeli, M.-L., Frontera, V., and Aurrand-Lions, M. (2013). Function of junctional adhesion molecules (JAMs) in leukocyte migration and homeostasis. Arch Immunol Ther Exp (Warsz.) 61, 15–23.

Arcangeli, M.-L., Frontera, V., Bardin, F., Obrados, E., Adams, S., Chabannon, C., Schiff, C., Mancini, S.J.C., Adams, R.H., and Aurrand-Lions, M. (2011). JAM-B regulates maintenance of hematopoietic stem cells in the bone marrow. Blood 118, 4609–4619.

Babbs, C.F., and Shi, R. (2013). Subtle paranodal injury slows impulse conduction in a mathematical model of myelinated axons. PloS one 8, e67767.

Bakhti, M., Snaidero, N., Schneider, D., Aggarwal, S., Möbius, W., Janshoff, A., Eckhardt, M., Nave, K.A., and Simons, M. (2013). Loss of electrostatic cell-surface repulsion mediates myelin membrane adhesion and compaction in the central nervous system. Proc Natl Acad Sci USA 110, 3143-3148.

Bechler, M.E., Byrne, L., and Ffrench-Constant, C. (2015). CNS Myelin Sheath Lengths Are an Intrinsic Property of Oligodendrocytes. Curr Biol 25, 2411–2416.

Bergles, D.E., Roberts, J.D., Somogyi, P., and Jahr, C.E. (2000). Glutamatergic synapses on oligodendrocyte precursor cells in the hippocampus. Nature 405, 187-191.

Bird, T.D., Farrell, D.F., and Sumi, S.M. (1978). Brain lipid composition of the shiverer mouse: (genetic defect in myelin development). J Neurochem 31, 387-391.

Bizzozero, O.A., and Howard, T.A. (2002). Myelin proteolipid protein-induced aggregation of lipid vesicles: efficacy of the various molecular species. Neurochem Res 27, 1269-1277.

Blinzinger, K., Anzil, A.P., and Müller, W. (1972). Myelinated nerve cell perikaryon in mouse spinal cord. Z Für Zellforsch Mikrosk Anat 128, 135–138.

Braak, E., Braak, H., and Strenge, H. (1977). The fine structure of myelinated nerve cell bodies in the bulbus olfactorius of man. Cell Tissue Res 182, 221–233.

Brinkmann, B.G., Agarwal, A., Sereda, M.W., Garratt, A.N., Müller, T., Wende, H., Stassart, R.M., Nawaz, S., Humml, C., Velanac, V., et al. (2008). Neuregulin-1/ErbB signaling serves distinct functions in myelination of the peripheral and central nervous system. Neuron 59, 581-595.

Brody, B.A., Kinney, H.C., Kloman, A.S., and Gilles, F.H. (1987). Sequence of central nervous system myelination in human infancy. I. An autopsy study of myelination. J Neuropathol Exp Neurol 46, 283-301.

Bunge, M.B., Bunge, R.P., and Pappas, G.D. (1962). Electron microscopic demonstration of connections between glia and myelin sheaths in the developing mammalian central nervous system. J Cell Biol 12, 448-453.

Bunge, R.P., Bunge, M.B., and Bates, M. (1989). Movements of the Schwann cell nucleus implicate progression of the inner (axon-related) Schwann cell process during myelination. J Cell Biol 109, 273-284.

Camu, W., and Henderson, C.E. (1992). Purification of embryonic rat motoneurons by panning on a monoclonal antibody to the low-affinity NGF receptor. J Neurosci Methods 44, 59–70.

Chang, A., Tourtellotte, W.W., Rudick, R., and Trapp, B.D. (2002). Premyelinating oligodendrocytes in chronic lesions of multiple sclerosis. N Engl J Med 346, 165–173.

Chang, K.J., and Rasband, M.N. (2013). Excitable domains of myelinated nerves: axon initial segments and nodes of Ranvier. Curr Top Membr 72, 159-192.

Chang, K.-J., Redmond, S.A., and Chan, J.R. (2016) Remodeling myelination: implications for mechanisms of neural plasticity. Nat Neurosci. 19(2): 190–197.

Chomiak, T., and Hu, B. (2009). What is the optimal value of the g-ratio for myelinated fibers in the rat CNS? A theoretical approach. PloS one 4, e7754.

Chong, S.Y.C., Rosenberg, S.S., Fancy, S.P.J., Zhao, C., Shen, Y.-A.A., Hahn, A.T., McGee, A.W., Xu, X., Zheng, B., Zhang, L.I., Rowitch, D.A., Franklin, R.J.M., Lu, Q.R., and Chan, J.R. (2012). Neurite outgrowth inhibitor Nogo-A establishes spatial segregation and extent of oligodendrocyte myelination. Proc Natl Acad Sci 109, 1299–1304.

Coetzee, T., Suzuki, K., Nave, K.A., and Popko, B. (1999). Myelination in the absence of galactolipids and proteolipid proteins. Mol Cell Neurosci 14, 41-51.

Cooper, M.H., and Beal, J.A. (1977). Myelinated granule cell bodies in the cerebellum of the monkey (Saimiri sciureus). Anat Rec 187, 249–255.

Cramer, P.E., Cirrito, J.R., Wesson, D.W., Lee, C.Y., Karlo, J.C., Zinn, A.E., Casali, B.T., Restivo, J.L., Goebel, W.D., James, M.J., Brunden, K.R., Wilson, D.A., and Landreth, G.E. (2012) ApoE-directed therapeutics rapidly clear β-amyloid and reverse deficits in AD mouse models. Science. Mar 23;335(6075):1503-6.

Czopka, T., ffrench-Constant, C., and Lyons, D.A. (2013). Individual oligodendrocytes have only a few hours in which to generate new myelin sheaths in vivo. Dev. Cell 25, 599-609.

de Hoz, L., and Simons, M. (2015). The emerging functions of oligodendrocytes in regulating neuronal network behaviour. BioEssays : news and reviews in molecular, cellular and developmental biology 37, 60-69.

Durafourt, B.A., Moore, C.S., Zammit, D.A., Johnson, T.A., Zaguia, F., Guiot, M.C., Bar-Or, A., and Antel, J.P. (2012) Comparison of polarization properties of human adult microglia and blood-derived macrophages. Glia. May;60(5):717-27.

Einheber, S., Zanazzi, G., Ching, W., Scherer, S., Milner, T.A., Peles, E., and Salzer, J.L. (1997). The axonal membrane protein Caspr, a homologue of neurexin IV, is a component of the septate-like paranodal junctions that assemble during myelination. J Cell Biol 139, 1495–1506.

Eisenbach, M., Kartvelishvily, E., Eshed-Eisenbach, Y., Watkins, T., Sorensen, A., Thomson, C., Ranscht, B., Barnett, S.C., Brophy, P., and Peles, E. (2009). Differential clustering of Caspr by oligodendrocytes and Schwann cells. J Neurosci Res. 87, 3492–3501.

Eshed-Eisenbach, Y., and Peles, E. (2013). The making of a node: a co-production of neurons and glia. Curr Opin Neurobiol 23, 1049-1056.

Fancy, S.P.J., Harrington, E.P., Yuen, T.J., Silbereis, J.C., Zhao, C., Baranzini, S.E., Bruce, C.C., Otero, J.J., Huang, E.J., Nusse, R., et al. (2011). Axin2 as regulatory and therapeutic target in newborn brain injury and remyelination. Nat Neurosci 14, 1009–1016.

Fields, R.D. (2008). White matter in learning, cognition and psychiatric disorders. Trends Neurosci 31, 361-370.

Foran, D.R., and Peterson, A.C. (1992). Myelin acquisition in the central nervous system of the mouse revealed by an MBP-Lac Z transgene. J Neurosci 12, 4890-4897.

Fraher, J.P. (1973). A quantitative study of anterior root fibres during early myelination. II. Longitudinal variation in sheath thickness and axon circumference. J Anat 115, 421-444.

Fraher, J.P. (1978). Quantitative studies on the maturation of central and peripheral parts of individual ventral motoneuron axons. I. Myelin sheath and axon calibre. J Anat 126, 509-533.

Franklin, R.J.M. (2002). Why does remyelination fail in multiple sclerosis? Nat Rev Neurosci 3, 705-714.

Franklin, R.J.M., and ffrench-Constant, C. (2008). Remyelination in the CNS: from biology to therapy. Nat Rev Neurosci 9, 839–855.

Galiano, M.R., Jha, S., Ho, T.S., Zhang, C., Ogawa, Y., Chang, K.J., Stankewich, M.C., Mohler, P.J., and Rasband, M.N. (2012). A distal axonal cytoskeleton forms an intra-axonal boundary that controls axon initial segment assembly. Cell 149, 1125-1139.

Geren, B.B. (1954). The formation from the Schwann cell surface of myelin in the peripheral nerves of chick embryos. Exp Cell Res 7, 558-562.

Gibson, E.M., Purger, D., Mount, C.W., Goldstein, A.K., Lin, G.L., Wood, L.S., Inema, I., Miller, S.E., Bieri, G., Zuchero, J.B., et al. (2014). Neuronal activity promotes oligodendrogenesis and adaptive myelination in the mammalian brain. Science 344, 1252304.

Goebbels, S., Oltrogge, J.H., Kemper, R., Heilmann, I., Bormuth, I., Wolfer, S., Wichert, S.P., Möbius, W., Liu, X., Lappe-Siefke, C., et al. (2010). Elevated phosphatidylinositol 3,4,5-trisphosphate in glia triggers cell-autonomous membrane wrapping and myelination. J Neurosci 30, 8953-8964.

Gravel, M., Peterson, J., Yong, V.W., Kottis, V., Trapp, B., and Braun, P.E. (1996). Overexpression of 2′,3′-cyclic nucleotide 3′-phosphodiesterase in transgenic mice alters oligodendrocyte development and produces aberrant myelination. Mol Cell Neurosci 7, 453-466.

Harauz, G., and Libich, D.S. (2009). The classic basic protein of myelin--conserved structural motifs and the dynamic molecular barcode involved in membrane adhesion and protein-protein interactions. Curr Protein Pept Sci 10, 196-215.

Harauz, G., Ladizhansky, V., and Boggs, J.M. (2009). Structural polymorphism and multifunctionality of myelin basic protein. Biochemistry 48, 8094-8104.

Hartline, D.K., and Colman, D.R. (2007). Rapid conduction and the evolution of giant axons and myelinated fibers. Curr Biol 17, R29-R35.

Hildebrand, C., Remahl, S., Persson, H., and Bjartmar, C. (1993). Myelinated nerve fibres in the CNS. Prog Neurobiol 40, 319-384.

Hines, J.H., Ravanelli, A.M., Schwindt, R., Scott, E.K., and Appel, B. (2015). Neuronal activity biases axon selection for myelination in vivo. Nat Neurosci 18, 683-689.

Hughes, E.G., Kang, S.H., Fukaya, M., and Bergles, D.E. (2013) Oligodendrocyte progenitors balance growth with self-repulsion to achieve homeostasis in the adult brain. Nat Neurosci 16(6):668-76.

Inoue, Y., Nakamura, R., Mikoshiba, K., and Tsukada, Y. (1981). Fine structure of the central myelin sheath in the myelin deficient mutant Shiverer mouse, with special reference to the pattern of myelin formation by oligodendroglia. Brain Res 219, 85-94.

Ioannidou, K., Anderson, K.I., Strachan, D., Edgar, J.M., and Barnett, S.C. (2012). Time-lapse imaging of the dynamics of CNS glial-axonal interactions in vitro and ex vivo. PloS one 7, e30775.

Jahn, O., Tenzer, S., and Werner, H.B. (2009). Myelin proteomics: molecular anatomy of an insulating sheath. Mol Neurobiol 40, 55-72.

Kattnig, D.R., Bund, T., Boggs, J.M., Harauz, G., and Hinderberger, D. (2012). Lateral self-assembly of 18.5-kDa myelin basic protein (MBP) charge component-C1 on membranes. Biochim Biophys Acta 1818, 2636-2647.

Kinney, H.C., Brody, B.A., Kloman, A.S., and Gilles, F.H. (1988). Sequence of central nervous system myelination in human infancy. II. Patterns of myelination in autopsied infants. J Neuropathol Exp Neurol 47, 217-234.

Klugmann, M., Schwab, M.H., Pühlhofer, A., Schneider, A., Zimmermann, F., Griffiths, I.R., and Nave, K.A. (1997). Assembly of CNS myelin in the absence of proteolipid protein. Neuron 18, 59-70.

Kotter, M.R., Li, W.W., Zhao, C., and Franklin, R.J. (2006) Myelin impairs CNS remyelination by inhibiting oligodendrocyte precursor cell differentiation. J Neurosci. 2006 Jan 4;26(1):328-32.

Kukley, M., Capetillo-Zarate, E., and Dietrich, D. (2007). Vesicular glutamate release from axons in white matter. Nat Neurosci 10, 311-320.

Lee, D.W., Banquy, X., Kristiansen, K., Kaufman, Y., Boggs, J.M., and Israelachvili, J.N. (2014). Lipid domains control myelin basic protein adsorption and membrane interactions between model myelin lipid bilayers. Proc Natl Acad Sci USA 111, E768-E775.

Lee, S., Chong, S.Y.C., Tuck, S.J., Corey, J.M., and Chan, J.R. (2013). A rapid and reproducible assay for modeling myelination by oligodendrocytes using engineered nanofibers. Nat Protoc 8, 771–782.

Lee, S., Leach, M.K., Redmond, S.A., Chong, S.Y., Mellon, S.H., Tuck, S.J., Feng, Z.Q., Corey, J.M., and Chan, J.R. (2012). A culture system to study oligodendrocyte myelination processes using engineered nanofibers. Nat Methods 9, 917-922.

Lee, X., Yang, Z., Shao, Z., Rosenberg, S.S., Levesque, M., Pepinsky, R.B., Qiu, M., Miller, R.H., Chan, J.R., and Mi, S. (2007). NGF regulates the expression of axonal LINGO-1 to inhibit oligodendrocyte differentiation and myelination. J Neurosci 27, 220–225.

Li, Q., Brus-Ramer, M., Martin, J.H., and McDonald, J.W. (2010). Electrical stimulation of the medullary pyramid promotes proliferation and differentiation of oligodendrocyte progenitor cells in the corticospinal tract of the adult rat. Neurosci Lett 479, 128-133.

Lin, S.C., and Bergles, D.E. (2004). Synaptic signaling between GABAergic interneurons and oligodendrocyte precursor cells in the hippocampus. Nat Neurosci 7, 24-32.

Liu, J., Dietz, K., DeLoyht, J.M., Pedre, X., Kelkar, D., Kaur, J., Vialou, V., Lobo, M.K., Dietz, D.M., Nestler, E.J., et al. (2012). Impaired adult myelination in the prefrontal cortex of socially isolated mice. Nat Neurosci 15, 1621-1623.

Lubetzki, C., Demerens, C., Anglade, P., Villarroya, H., Frankfurter, A., Lee, V.M., and Zalc, B. (1993). Even in culture, oligodendrocytes myelinate solely axons. Proc Natl Acad Sci USA 90, 6820–6824.

Makinodan, M., Rosen, K.M., Ito, S., and Corfas, G. (2012). A critical period for social experience-dependent oligodendrocyte maturation and myelination. Science 337, 1357-1360.

McKenzie, I.A., Ohayon, D., Li, H., de Faria, J.P., Emery, B., Tohyama, K., and Richardson, W.D. (2014). Motor skill learning requires active central myelination. Science 346, 318-322.

Mei, F., Fancy, S.P.J., Shen, Y.-A.A., Niu, J., Zhao, C., Presley, B., Miao, E., Lee, S., Mayoral, S.R., Redmond, S.A., et al. (2014). Micropillar arrays as a high-throughput screening platform for therapeutics in multiple sclerosis. Nat Med 20, 954–960.

Mei, L., and Nave, K.A. (2014). Neuregulin-ERBB signaling in the nervous system and neuropsychiatric diseases. Neuron 83, 27-49.

Mensch, S., Baraban, M., Almeida, R., Czopka, T., Ausborn, J., El Manira, A., and Lyons, D.A. (2015). Synaptic vesicle release regulates myelin sheath number of individual oligodendrocytes in vivo. Nat Neurosci 18, 628-630.

Mi, S., Miller, R.H., Lee, X., Scott, M.L., Shulag-Morskaya, S., Shao, Z., Chang, J., Thill, G., Levesque, M., Zhang, M., et al. (2005). LINGO-1 negatively regulates myelination by oligodendrocytes. Nat Neurosci 8, 745–751.

Mirsky, R., Winter, J., Abney, E.R., Pruss, R.M., Gavrilovic, J., and Raff, M.C. (1980). Myelin-specific proteins and glycolipids in rat Schwann cells and oligodendrocytes in culture. J Cell Biol 84, 483-494.

Möbius, W., Cooper, B., Kaufmann, W.A., Imig, C., Ruhwedel, T., Snaidero, N., Saab, A.S., and Varoqueaux, F. (2010). Electron microscopy of the mouse central nervous system. Methods Cell Biol 96, 475-512.

Möbius, W., Patzig, J., Nave, K.A., and Werner, H.B. (2008). Phylogeny of proteolipid proteins: divergence, constraints, and the evolution of novel functions in myelination and neuroprotection. Neuron Glia Biol 4, 111-127.

Molofsky, A.V., Kelley, K.W., Tsai, H.-H., Redmond, S.A., Chang, S.M., Madireddy, L., Chan, J.R., Baranzini, S.E., Ullian, E.M., and Rowitch, D.H. (2014). Astrocyte-encoded positional cues maintain sensorimotor circuit integrity. Nature 509, 189–194.

Nave, K.A., and Salzer, J.L. (2006). Axonal regulation of myelination by neuregulin 1. Curr Opin Neurobiol 16, 492-500.

Nawaz, S., Kippert, A., Saab, A.S., Werner, H.B., Lang, T., Nave, K.A., and Simons, M. (2009). Phosphatidylinositol 4,5-bisphosphate-dependent interaction of myelin basic protein with the plasma membrane in oligodendroglial cells and its rapid perturbation by elevated calcium. J Neurosci 29, 4794-4807.

Nawaz, S., Sánchez, P., Schmitt, S., Snaidero, N., Mitkovski, M., Velte, C., Brückner, B.R., Alexopoulos, I., Czopka, T., Jung, S.Y., et al. (2015). Actin filament turnover drives leading edge growth during myelin sheath formation in the central nervous system. Dev Cell 34, 139-151.

Normand, E.A., and Rasband, M.N. (2015). Subcellular patterning: axonal domains with specialized structure and function. Dev Cell 32, 459-468.

Pajevic, S., Basser, P.J., and Fields, R.D. (2014). Role of myelin plasticity in oscillations and synchrony of neuronal activity. Neuroscience 276, 135-147.

Palaniyar, N., Semotok, J.L., Wood, D.D., Moscarello, M.A., and Harauz, G. (1998). Human proteolipid protein (PLP) mediates winding and adhesion of phospholipid membranes but prevents their fusion. Biochim Biophys Acta 1415, 85-100.

Peddie, C.J., and Collinson, L.M. (2014). Exploring the third dimension: volume electron microscopy comes of age. Micron 61, 9-19.

Pedraza, L., Huang, J.K., and Colman, D. (2009). Disposition of axonal caspr with respect to glial cell membranes: Implications for the process of myelination. J Neurosci Res. 87, 3480–3491.

Pérez-Cerdá, F., Sánchez-Gómez, M.V., and Matute, C. (2015). Pío del Río Hortega and the discovery of the oligodendrocytes. Front Neuroanat 9, 92.

Peters, A. (1964). Further observations on the structure of myelin sheaths in the central nervous system. J Cell Biol 20, 281-296.

Piaton, G., Gould, R.M., and Lubetzki, C. (2010). Axon-oligodendrocyte interactions during developmental myelination, demyelination and repair. J Neurochem 114, 1243-1260.

Privat, A., Jacque, C., Bourre, J.M., Dupouey, P., and Baumann, N. (1979). Absence of the major dense line in myelin of the mutant mouse "shiverer". Neurosci Lett 12, 107-112.

Ramón y Cajal, S. (1928). Degeneration & Regeneration of the Nervous System (London: Oxford University Press).

Ranscht, B., Clapshaw, P.A., Price, J., Noble, M., and Seifert, W. (1982). Development of oligodendrocytes and Schwann cells studied with a monoclonal antibody against galactocerebroside. Proc Natl Acad Sci USA 79, 2709–2713.

Redmond, S.A. and Chan, J.R. (2012) Revitalizing remyelination--the answer is circulating. Science 336(6078):161-2.

Redmond S.A., Mei F., Eshed-Eisenbach Y., Osso L.A., Leshkowitz, D., Shen Y.-A.A., Kay J.-N., Aurrand-Lions M., Lyons D.A., Peles E., and Chan J.R. (2016) JAM2 inhibits somatodendritic myelination by oligodendrocytes. Neuron *in press*.

Remahl, S., and Hildebrand, C. (1985). Myelinated non-axonal neuronal elements in the feline olfactory bulb lack sites with a nodal structural differentiation. Brain Res 325, 1–11.

Richardson, W.D., Young, K.M., Tripathi, R.B., and McKenzie, I. (2011). NG2-glia as multipotent neural stem cells: fact or fantasy? Neuron 70, 661-673.

Roberts, A., Pimentel, H., Trapnell, C., and Pachter, L. (2011). Identification of novel transcripts in annotated genomes using RNA-Seq. Bioinforma Oxf Engl 27, 2325–2329.

Robertson, J.D. (1955). The ultrastructure of adult vertebrate peripheral myelinated nerve fibers in relation to myelinogenesis. J Biophys Biochem Cytol 1, 271-278.

Rosenberg, S.S., Kelland, E.E., Tokar, E., De La Torre, A.R., and Chan, J.R. (2008). The geometric and spatial constraints of the microenvironment induce oligodendrocyte differentiation. Proc Natl Acad Sci USA 105, 14662-14667.

Rosenbluth, J. (1980). Central myelin in the mouse mutant shiverer. J Comp Neurol 194, 639-648.

Ruckh, J.M., Zhao, J.-W., Shadrach, J.L., van Wijngaarden, P., Rao, T.N., Wagers, A.J., and Franklin, R.J.M. (2012). Rejuvenation of Regeneration in the Aging Central Nervous System. Cell Stem Cell 10, 96–103.

Salzer, J.L. (2015). Schwann cell myelination. Cold Spring Harb Perspect Biol 7, a020529.

Schnaar, R.L., Gerardy-Schahn, R., and Hildebrandt, H. (2014). Sialic acids in the brain: gangliosides and polysialic acid in nervous system development, stability, disease, and regeneration. Physiol Rev 94, 461-518.

Seidl, A.H. (2014). Regulation of conduction time along axons. Neuroscience 276, 126-134.

Seidl, A.H., Rubel, E.W., and Harris, D.M. (2010). Mechanisms for adjusting interaural time differences to achieve binaural coincidence detection. J Neurosci 30, 70-80.

Sharma, K., Schmitt, S., Bergner, C.G., Tyanova, S., Kannaiyan, N., Manrique-Hoyos, N., Kongi, K., Cantuti, L., Hanisch, U.-K., Philips, M.-A., et al. (2015). Cell type- and brain region-resolved mouse brain proteome. Nat. Neurosci. 18, 1819–1831.

Shechter, R., London, A., Varol, C., Raposo, C., Cusimano, M., Yovel, G., Rolls, A., Mack, M., Pluchino, S., Martino, G., Jung, S., and Schwartz M. (2009). Infiltrating blood-derived macrophages are vital cells playing an anti-inflammatory role in recovery from spinal cord injury in mice. PLoS Med. Jul;6(7):e1000113.

Shen, S., Sandoval, J., Swiss, V.A., Li, J., Dupree, J., Franklin, R.J., and Casaccia-Bonnefil, P. (2008). Age-dependent epigenetic control of differentiation inhibitors is critical for remyelination efficiency. Nat. Neurosci. Sep;11(9):1024-34.

Smith, K.M., Boyle, K.A., Madden, J.F., Dickinson, S.A., Jobling, P., Callister, R.J., Hughes, D.I., and Graham, B.A. (2015). Functional heterogeneity of calretinin-expressing neurons in the mouse superficial dorsal horn: implications for spinal pain processing. J. Physiol. 593, 4319–4339.

Snaidero, N., and Simons, M. (2014). Myelination at a glance. J Cell Sci 127, 2999-3004.

Snaidero, N., Möbius, W., Czopka, T., Hekking, L.H., Mathisen, C., Verkleij, D., Goebbels, S., Edgar, J., Merkler, D., Lyons, D.A., et al. (2014). Myelin membrane wrapping of CNS axons by PI(3,4,5)P3-dependent polarized growth at the inner tongue. Cell 156, 277-290.

Sobottka, B., Ziegler, U., Kaech, A., Becher, B., and Goebels, N. (2011). CNS live imaging reveals a new mechanism of myelination: the liquid croissant model. Glia 59, 1841-1849.

Taveggia, C., Feltri, M.L., and Wrabetz, L. (2010). Signals to promote myelin formation and repair. Nat Rev Neurol 6, 276-287.

Tomassy, G.S., Berger, D.R., Chen, H.H., Kasthuri, N., Hayworth, K.J., Vercelli, A., Seung, H.S., Lichtman, J.W., and Arlotta, P. (2014). Distinct profiles of myelin distribution along single axons of pyramidal neurons in the neocortex. Science 344, 319-324.

Trapnell, C., Pachter, L., and Salzberg, S.L. (2009). TopHat: discovering splice junctions with RNA-Seq. Bioinforma. Oxf. Engl. 25, 1105–1111.

Trapnell, C., Williams, B.A., Pertea, G., Mortazavi, A., Kwan, G., van Baren, M.J., Salzberg, S.L., Wold, B.J., and Pachter, L. (2010). Transcript assembly and quantification by RNA-Seq reveals unannotated transcripts and isoform switching during cell differentiation. Nat. Biotechnol. 28, 511–515.

Trapp, B.D., and Nave, K.-A. (2008). Multiple sclerosis: an immune or neurodegenerative disorder? Annu. Rev. Neurosci. 31, 247–269.

Villeda, S.A., Luo, J., Mosher, K.I., Zou, B., Britschgi, M., Bieri, G., Stan, T.M., Fainberg, N., Ding, Z., Eggel, A., Lucin, K.M., Czirr, E., Park, J.S., Couillard-Després, S., Aigner, L., Li, G., Peskind, E.R., Kaye, J.A., Quinn, J.F., Galasko, D.R., Xie, X.S., Rando, T.A., and Wyss-Coray, T. (2011) The ageing systemic milieu negatively regulates neurogenesis and cognitive function. Nature. 2011 Aug 31;477(7362):90-4.

Virchow, R. (1854). Über das ausgebreitete Vorkommen einer dem Nervenmark analogen Substanz in den tierischen Geweben. Virchows Arch Pathol Anat 6, 562-572.

Wang, S., and Young, K.M. (2014). White matter plasticity in adulthood. Neuroscience 276, 148-160.

Wang, S.S., Shultz, J.R., Burish, M.J., Harrison, K.H., Hof, P.R., Towns, L.C., Wagers, M.W., and Wyatt, K.D. (2008). Functional trade-offs in white matter axonal scaling. J Neurosci 28, 4047-4056.

Watkins, T.A., Emery, B., Mulinyawe, S., and Barres, B.A. (2008). Distinct stages of myelination regulated by γ-secretase and astrocytes in a rapidly myelinating CNS coculture system. Neuron 60, 555-569.

Waxman, S.G. (1980). Determinants of conduction velocity in myelinated nerve fibers. Muscle & nerve 3, 141-150.

Waxman, S.G. (1997). Axon-glia interactions: building a smart nerve fiber. Curr Biol 7, R406-R410.

Waxman, S.G., and Swadlow, H.A. (1976). Ultrastructure of visual callosal axons in the rabbit. Exp Neurol 53, 115-127.

Webster, H.D. (1971). The geometry of peripheral myelin sheaths during their formation and growth in rat sciatic nerves. J Cell Biol 48, 348-367.

Weskamp, G., and Reichardt, L.F. (1991). Evidence that biological activity of NGF is mediated through a novel subclass of high affinity receptors. Neuron 6, 649–663.

Yeung, M.S., Zdunek, S., Bergmann, O., Bernard, S., Salehpour, M., Alkass, K., Perl, S., Tisdale, J., Possnert, G., Brundin, L., et al. (2014). Dynamics of oligodendrocyte generation and myelination in the human brain. Cell 159, 766-774.

Yin, X., Peterson, J., Gravel, M., Braun, P.E., and Trapp, B.D. (1997). CNP overexpression induces aberrant oligodendrocyte membranes and inhibits MBP accumulation and myelin compaction. J Neurosci Res 50, 238-247.

Yoshimura, T., and Rasband, M.N. (2014). Axon initial segments: diverse and dynamic neuronal compartments. Curr Opin Neurobiol 27, 96-102.

Yuen, T.J., Silbereis, J.C., Griveau, A., Chang, S.M., Daneman, R., Fancy, S.P.J., Zahed, H., Maltepe, E., and Rowitch, D.H. (2014). Oligodendrocyte-encoded HIF function couples postnatal myelination and white matter angiogenesis. Cell 158, 383–396.

Zalc, B., Goujet, D., and Colman, D. (2008). The origin of the myelination program in vertebrates. Curr Biol 18, R511–R512.

Zalc, B., Goujet, D., and Colman, D. (2008). The origin of the myelination program in vertebrates. Curr Biol 18, R511-R512.

Zatorre, R.J., Fields, R.D., and Johansen-Berg, H. (2012). Plasticity in gray and white: neuroimaging changes in brain structure during learning. Nat Neurosci 15, 528-536.

Ziskin, J.L., Nishiyama, A., Rubio, M., Fukaya, M., and Bergles, D.E. (2007). Vesicular release of glutamate from unmyelinated axons in white matter. Nat Neurosci 10, 321-330.

Zuchero, J.B., Fu, M.M., Sloan, S.A., Ibrahim, A., Olson, A., Zaremba, A., Dugas, J.C., Wienbar, S., Caprariello, A.V., Kantor, C., et al. (2015). CNS myelin wrapping is driven by actin disassembly. Dev Cell 34, 152-167.

Publishing Agreement

It is the policy of the University to encourage the distribution of all theses, dissertations, and manuscripts. Copies of all UCSF theses, dissertations, and manuscripts will be routed to the library via the Graduate Division. The library will make all theses, dissertations, and manuscripts accessible to the public and will preserve these to the best of their abilities, in perpetuity.

Please sign the following statement:

I hereby grant permission to the Graduate Division of the University of California, San Francisco to release copies of my thesis, dissertation, or manuscript to the Campus Library to provide access and preservation, in whole or in part, in perpetuity.

Author Signature

4 August 2016

Date